INTERNATIONAL JOURNAL OF
NUMERICAL ANALYSIS AND MODELING
Volume 13, Number 1, Pages 90–113

NUMERICAL ANALYSIS AND TESTING OF A FULLY DISCRETE, DECOUPLED PENALTY-PROJECTION ALGORITHM FOR MHD IN ELSÄSSER VARIABLE

MINE AKBAS, SONGUL KAYA, MUHAMMAD MOHEBUJJAMAN, AND LEO G. REBHOLZ

(Communicated by Max Gunzburger)

Abstract. We consider a fully discrete, efficient algorithm for magnetohydrodynamic (MHD) flow that is based on the Elsässer variable formulation and a timestepping scheme that decouples the MHD system but still provides unconditional stability with respect to the timestep. We prove stability and optimal convergence of the scheme, and also connect the scheme to one based on handling each decoupled system with a penalty-projection method. Numerical experiments are given which verify all predicted convergence rates of our analysis on some analytical test problems, show the results of the scheme on a set of channel flow problems match well the results found when the computation is done with MHD in primitive variable, and finally show the scheme performs well on a channel flow over a step.

Key words. Magnetohydrodynamics, Elsässer variables, Penalty-projection method, finite element method

1. Introduction

We consider the efficient and accurate numerical approximation of magnetohydrodynamic (MHD) flow, which is governed by the system of evolution equations [19, 5]

$$u_t + (u\cdot\nabla)u - s(B\cdot\nabla)B - \nu\Delta u + \nabla p = f, \tag{1}$$

$$\nabla\cdot u = 0, \tag{2}$$

$$B_t + (u\cdot\nabla)B - (B\cdot\nabla)u - \nu_m\Delta B + \nabla\lambda = \nabla\times g, \tag{3}$$

$$\nabla\cdot B = 0, \tag{4}$$

in $\Omega\times(0,T)$, where Ω is the domain of the fluid, u is the velocity of the fluid, p is a modified pressure, B is the magnetic field, s is the coupling number, ν is the kinematic viscosity, ν_m is the magnetic resistivity, f is the body force, and $\nabla\times g$ is the forcing on the magnetic field. The physical principles governing such flows are that when an electrically conducting fluid moves in a magnetic field, the magnetic field induces currents in the fluid, which in turn creates forces on the fluid and also alters the magnetic field. In the recent years, the study of MHD flows has become important due to applications in, e.g. astrophysics and geophysics [17, 23, 12, 10, 4, 6], liquid metal cooling of nuclear reactors [3, 15, 26], and process metallurgy [8].

A fundamental difficulty in simulating MHD flow is solving the fully coupled linear systems that arise in common discretizations of (1)-(4). It is an open problem how to decouple the equations in an unconditionally stable way (with respect to the timestep size), and thus timestepping methods that decouple the equations are prone to unstable behavior without using excessively small timestep sizes. To

Received by the editors November 17, 2015.

1991 *Mathematics Subject Classification.* 65M60, 76W05.

confront this issue, an excellent idea was presented by Trenchea in [27]: if one rewrites the MHD system in terms of Elsässer variables (defined below), then an unconditionally stable, decoupled, timestepping algorithm can be created. Analysis of this algorithm in a semidiscrete setting (temporal discretization only) with a defect correction method was performed in [28], but no numerical experiments were performed beyond convergence rate verification. The purpose of this paper is 1) to analyze and test Trenchea's algorithm in a fully discrete setting, i.e. together with a finite element spatial discretization, 2) to extend the algorithm and analysis to a more efficient class of timestepping algorithms (penalty-projection type), and 3) test the algorithms on some benchmark problems and compare to simulations with primitive variables.

The Elsässer formulation of MHD was first proposed by W. Elsässer in 1950 [11], and since then has been used in several analytical studies, e.g. [25, 9, 22]. To derive it, begin by splitting the magnetic field into two parts, $\sqrt{s}B =: \sqrt{s}B_0 + \sqrt{s}b$ (mean and fluctuation, respectively), with $B_0 = B_0(t)$. For boundary conditions, we assume the Dirichlet condition $B = B_0$ on $\partial\Omega$, and homogeneous Dirichlet conditions for the velocity, $u = 0$, and magnetic field fluctuations, $b = 0$. The system (1)-(4) can now be written as

$$u_t + (u\cdot\nabla)u - s(B_0\cdot\nabla)b - s(b\cdot\nabla)b - \nu\Delta u + \nabla p = f, \tag{5}$$
$$\nabla\cdot u = 0, \tag{6}$$
$$b_t + (u\cdot\nabla)b - (B_0\cdot\nabla)u - (b\cdot\nabla)u - \nu_m\Delta b + \nabla\lambda = \nabla\times g - \frac{dB_0}{dt}, \tag{7}$$
$$\nabla\cdot b = 0. \tag{8}$$

Rescaling (7) by $\sqrt{s}$, adding (subtracting) (5) to (from) (7) and setting $f_1 := f + \nabla\times g - \frac{dB_0}{dt}$, $f_2 := f - \sqrt{s}(\nabla\times g + \frac{dB_0}{dt})$, $q := p + \sqrt{s}\lambda$ and $r := p - \sqrt{s}\lambda$ gives

$$\begin{aligned}
(u+\sqrt{s}b)_t + (u\cdot\nabla)(u+\sqrt{s}b) - (\sqrt{s}B_0\cdot\nabla)(u+\sqrt{s}b)&\\
-(\sqrt{s}b\cdot\nabla)(u+\sqrt{s}b) - \nu\Delta u - \nu_m\Delta(\sqrt{s}b) + \nabla q &= f_1,\\
\nabla\cdot(u+\sqrt{s}b) &= 0,\\
(u-\sqrt{s}b)_t + (u\cdot\nabla)(u-\sqrt{s}b) + (\sqrt{s}B_0\cdot\nabla)(u-\sqrt{s}b)&\\
+(\sqrt{s}b\cdot\nabla)(u-\sqrt{s}b) - \nu\Delta u + \nu_m\Delta(\sqrt{s}b) + \nabla r &= f_2,\\
\nabla\cdot(u-\sqrt{s}b) &= 0.
\end{aligned}$$

Now defining $v = u + \sqrt{s}b$, $w = u - \sqrt{s}b$, $\tilde{B}_0 = \sqrt{s}B_0$ produces the Elsässer formulation

$$v_t + w\cdot\nabla v - (\tilde{B}_0\cdot\nabla)v + \nabla q - \frac{\nu+\nu_m}{2}\Delta v - \frac{\nu-\nu_m}{2}\Delta w = f_1, \tag{9}$$
$$\nabla\cdot v = 0, \tag{10}$$
$$w_t + v\cdot\nabla w + (\tilde{B}_0\cdot\nabla)w + \nabla r - \frac{\nu+\nu_m}{2}\Delta w - \frac{\nu-\nu_m}{2}\Delta v = f_2, \tag{11}$$
$$\nabla\cdot w = 0. \tag{12}$$

This paper is arranged as follows. In section 2, we provide notation and mathematical preliminaries that will allow for a smooth analysis to follow. Section 3 presents the fully discrete scheme, and proves stability and convergence for it. Section 4 presents a penalty-projection variation of the scheme, and proves it is equivalent to the scheme of Section 3 when the the penalty parameter is large. Section 5 presents numerical experiments and conclusions are drawn in section 6.

2. Notation and Preliminaries

In this paper, we assume that $\Omega \subset \mathbb{R}^d, d \in 2,3$, is a polygonal or polyhedral domain with boundary $\partial\Omega$. We denote the usual $L^2(\Omega)$ norm and its inner product by $\|.\|$ and $(.,.)$ respectively. The $L^p(\Omega)$ norms and the Sobolev $W_p^k(\Omega)$ norms are denoted by $\|.\|_{L^p}$ and $\|.\|_{W_p^k(\Omega)}$ respectively for $k \in \mathbb{N}, 1 \leq p \leq \infty$. In particular, $H^k(\Omega)$ is used to represent the Sobolev space $W_2^k(\Omega)$. $\|.\|_{H^k}$ and $|.|_k$ denote the norm and the seminorm in $H^k(\Omega)$.

For X being a normed function space in $\Omega, L^p(0,t;X)$ is the space of all functions defined on $(0,t) \times \Omega$ for which the norm

$$\|u\|_{L^p(0,t;X)} = \left(\int_0^t \|u\|_X^p dt\right)^{1/p}, p \in [1,\infty)$$

is finite. For $p = \infty$, the usual modification is used in the definition of this space.

The natural function spaces for our problem are

$$X := H_0^1(\Omega) = \{v \in (L^2(\Omega))^d : \nabla v \in L^2(\Omega)^{d\times d}, v = 0 \text{ on } \partial\Omega\},$$

$$Q := L_0^2(\Omega) = \{q \in L^2(\Omega) : \int_\Omega q \ dx = 0\},$$

$$Y := \{v \in H^1(\Omega) : v \cdot n = 0 \text{ on } \partial\Omega\}$$

where n denote the outward unit normal vector normal to the boundary $\partial\Omega$. For f an element in the dual space of X, its norm is defined by

$$\|f\|_{-1} = \sup_{v\in X} \frac{\|(f,v)\|}{\|\nabla v\|}.$$

The space of divergence free functions is given by

$$V := \{v \in X : (\nabla \cdot v, q) = 0, \forall q \in Q\}$$

The Poincaré-Friedrichs' inequality will be used frequently throughout our analysis: For $v \in X$,

$$\|v\| \leq C\|\nabla v\|, \quad C = C(\Omega).$$

We define the trilinear form

$$b^*(u,v,w) := \frac{1}{2}((u\cdot\nabla v, w) - (u \cdot \nabla w, v)), \forall u \in V \text{and } \forall v,w \in X.$$

Note that $b^*(u,v,w)$ is skew symmetric and $b^*(u,v,v) = 0$. Moreover, $b^*(u,v,w)$ satisfies the following bound, [14],

$$|b^*(u,v,w)| \leq C(\Omega)\|\nabla u\|\|\nabla v\|\|\nabla w\|, \text{ for any } u,v,w \in X. \tag{13}$$

The following lemma for discrete Gronwall inequality was proven in [16].

Lemma 2.1. *Let Δt, B, a_n, b_n, c_n, d_n for integers $n \geq 0$ be non-negative numbers such that for $M \geq 1$. If*

$$a_M + \Delta t \sum_{n=0}^{M} b_n \leq \Delta t \sum_{n=0}^{M-1} d_n a_n + \Delta t \sum_{n=0}^{M} c_n + B \quad \text{for } M \geq 0,$$

then for all $\Delta t > 0$,

$$a_M + \Delta t \sum_{n=0}^{M} b_n \leq exp\left(\Delta t \sum_{n=0}^{M-1} d_n\right)\left(\Delta t \sum_{n=0}^{M} c_n + B\right) \quad \text{for } M \geq 0.$$

Let $X^h \subset X$, $Q^h \subset Q$ denote conforming velocity, pressure finite element spaces based on an edge to edge triangulations of Ω with maximum triangle diameter h. The velocity-pressure FEM spaces (X^h, Q^h) are assumed to satisfy the usual discrete inf-sup condition for stability of the discrete pressure:

$$\inf_{q^h \in Q^h} \sup_{v^h \in X^h} \frac{(q^h, \nabla \cdot v^h)}{\|q^h\| \|\nabla v^h\|} \geq \beta > 0, \tag{14}$$

where β is independent of h.

To help simplify a very technical analysis, we choose $(X_h, Q_h) = (P_k, P_{k-1}^{disc})$ Scott-Vogelius finite element pairs to approximate velocity-pressure spaces, which are known to fulfill inf-sup condition under certain restrictions on the mesh and polynomial degree, e.g. [2, 24, 30, 29]. However, our analysis can be extended without difficulty (but with more terms) to any inf-sup stable element choice. We have the following approximation properties typical of piecewise polynomials of degree $(k, k-1)$, [7], hold for (X_h, Q_h):

$$\inf_{v^h \in X^h} \|u - v^h\| \leq Ch^{k+1}|u|_{k+1}, \quad u \in H^{k+1}(\Omega), \tag{15}$$

$$\inf_{v^h \in X^h} \|\nabla(u - v^h)\| \leq Ch^{k}|u|_{k+1}, \quad u \in H^{k+1}(\Omega), \tag{16}$$

$$\inf_{q^h \in Q^h} \|p - q^h\| \leq Ch^{k}|p|_{k}, \quad p \in H^{k}(\Omega). \tag{17}$$

The discrete divergence free subspace of X^h is

$$V^h := \{v^h \in X^h : (\nabla \cdot v^h, q^h) = 0, \text{ for all } q^h \in Q^h\}.$$

With the use of Scott-Vogelius finite element pairs, V_h is conforming to V, i.e., $V_h \subset V$ and the functions in V_h are divergence-free pointwise.

3. Fully discrete scheme and analysis

In this section, we present and analyze a fully discrete scheme for (9)-(12).

Algorithm 3.1. *(Fully Coupled Scheme): Let $f_1, f_2 \in L^\infty(0, T; H^{-1}(\Omega))$ and time step $\Delta t > 0$ and end time $T > 0$ be given. Set $M = T/\Delta t$ and start with $\tilde{v}^0 = v(0), \tilde{w}^0 = w(0) \in H^2 \cup V$. For all $n = 0, 1, ..., M-1$, compute $(v_h^{n+1}, w_h^{n+1}) \in V_h \times V_h$ satisfying for all $(\chi_h,\ l_h) \in V_h \times V_h$,*

$$\begin{aligned}&\left(\frac{v_h^{n+1} - v_h^n}{\Delta t}, \chi_h\right) + (w_h^n \cdot \nabla v_h^{n+1}, \chi_h) - (\tilde{B}_0(t^{n+1}) \cdot \nabla v_h^{n+1}, \chi_h)\\ &+ \frac{\nu + \nu_m}{2}(\nabla v_h^{n+1}, \nabla \chi_h) + \frac{\nu - \nu_m}{2}(\nabla w_h^n, \nabla \chi_h) = (f_1(t^{n+1}), \chi_h),\end{aligned} \tag{18}$$

and

$$\begin{aligned}&\left(\frac{w_h^{n+1} - w_h^n}{\Delta t}, l_h\right) + (v_h^n \cdot \nabla w_h^{n+1}, l_h) + (\tilde{B}_0(t^{n+1}) \cdot \nabla w_h^{n+1}, l_h)\\ &+ \frac{\nu + \nu_m}{2}(\nabla w_h^{n+1}, \nabla l_h) + \frac{\nu - \nu_m}{2}(\nabla v_h^n, \nabla l_h) = (f_2(t^{n+1}), l_h).\end{aligned} \tag{19}$$

Even though the scheme is decoupled into 2 sub-problems, it is unconditionally stable with respect to the timestep size. We prove this in the following lemma.

Lemma 3.1. *Suppose $f_1, f_2 \in L^\infty(0,T;H^{-1}(\Omega))$, $v_h^0, w_h^0 \in H^1(\Omega)$. Then for any $\Delta t > 0$, solutions to (18)-(19) satisfy*

$$\begin{aligned}
&\|v_h^M\|^2 + \|w_h^M\|^2 + \frac{(\nu-\nu_m)^2}{2(\nu+\nu_m)}\Delta t\left(\|\nabla v_h^M\|^2 + \|\nabla w_h^M\|^2\right) \\
&+ \frac{\nu\nu_m}{\nu+\nu_m}\Delta t \sum_{n=0}^{M-1}\left(\|\nabla v_h^{n+1}\|^2 + \|\nabla w_h^{n+1}\|^2\right) \le \frac{(\nu-\nu_m)^2}{2(\nu+\nu_m)}\left(\|\nabla v_h^0\|^2 + \|\nabla w_h^0\|^2\right) \\
&\qquad + \|v_h^0\|^2 + \|w_h^0\|^2 + \frac{\nu+\nu_m}{\nu\nu_m}\Delta t \sum_{n=0}^{M-1}\left(\|f_1(t^{n+1})\|_{-1}^2 + \|f_2(t^{n+1})\|_{-1}^2\|\right).
\end{aligned}$$

Proof. Taking $\chi_h = v_h^{n+1}$ in (18), $l_h = w_h^{n+1}$ in (19), and using the polarization identity

$$(b-a, b) = \frac{1}{2}(\|b-a\|^2 + \|b\|^2 - \|a\|^2),$$

gives

$$\begin{aligned}
(20)\quad &\frac{1}{2\Delta t}\left(\|v_h^{n+1} - v_h^n\|^2 + \|v_h^{n+1}\|^2 - \|v_h^n\|^2\right) + \frac{\nu+\nu_m}{2}\|\nabla v_h^{n+1}\|^2 \\
&\qquad + \frac{\nu-\nu_m}{2}(\nabla w_h^n, \nabla v_h^{n+1}) = (f_1(t^{n+1}), v_h^{n+1}),
\end{aligned}$$

and

$$\begin{aligned}
(21)\quad &\frac{1}{2\Delta t}\left(\|w_h^{n+1} - w_h^n\|^2 + \|w_h^{n+1}\|^2 - \|w_h^n\|^2\right) + \frac{\nu+\nu_m}{2}\|\nabla w_h^{n+1}\|^2 \\
&\qquad + \frac{\nu-\nu_m}{2}(\nabla v_h^n, \nabla w_h^{n+1}) = (f_2(t^{n+1}), w_h^{n+1}).
\end{aligned}$$

Adding (20) and (21) yields

$$\begin{aligned}
&\frac{1}{2\Delta t}\left(\|v_h^{n+1}\|^2 + \|w_h^{n+1}\|^2 - (\|v_h^n\|^2 + \|w_h^n\|^2) + \|v_h^{n+1} - v_h^n\|^2 + \|w_h^{n+1} - w_h^n\|^2\right) \\
&+ \frac{\nu+\nu_m}{2}(\|\nabla v_h^{n+1}\|^2 + \|\nabla w_h^{n+1}\|^2) + \frac{\nu-\nu_m}{2}\left((\nabla w_h^n, v_h^{n+1}) + (\nabla v_h^n, \nabla w_h^{n+1})\right) \\
&\qquad = (f_1(t^{n+1}), v_h^{n+1}) + (f_2(t^{n+1}), w_h^{n+1}),
\end{aligned}$$

then using Cauchy-Schwarz's inequality on the right hand side provides

$$\begin{aligned}
&\frac{1}{2\Delta t}\left(\|v_h^{n+1}\|^2 + \|w_h^{n+1}\|^2 - (\|v_h^n\|^2 + \|w_h^n\|^2) + \|v_h^{n+1} - v_h^n\|^2 + \|w_h^{n+1} - w_h^n\|^2\right) \\
&+ \frac{\nu+\nu_m}{2}(\|\nabla v_h^{n+1}\|^2 + \|\nabla w_h^{n+1}\|^2) \le \left|\frac{\nu-\nu_m}{2}\right|\left(\|\nabla w_h^n\|\|\nabla v_h^{n+1}\| + \|\nabla v_h^n\|\|\nabla w_h^{n+1}\|\right) \\
&\qquad + \|f_1(t^{n+1})\|_{-1}\|\nabla v_h^{n+1}\| + \|f_2(t^{n+1})\|_{-1}\|\nabla w_h^{n+1}\|.
\end{aligned}$$

After application of Young's inequality $ab \le \frac{\epsilon}{2}a^2 + \frac{1}{2\epsilon}b^2$ with $\epsilon = \frac{\nu+\nu_m}{2}$, we obtain

$$\begin{aligned}
(22)\quad &\frac{1}{2\Delta t}(\|v_h^{n+1}\|^2 + \|w_h^{n+1}\|^2 - (\|v_h^n\|^2 + \|w_h^n\|^2) + \|v_h^{n+1} - v_h^n\|^2 \\
&\qquad + \|w_h^{n+1} - w_h^n\|^2) + \frac{\nu+\nu_m}{2}\left(\|\nabla v_h^{n+1}\|^2 + \|\nabla w_h^{n+1}\|^2\right) \\
&\le \frac{\nu+\nu_m}{4}\|\nabla v_h^{n+1}\|^2 + \frac{(\nu-\nu_m)^2}{4(\nu+\nu_m)}\|\nabla w_h^n\|^2 + \frac{\nu+\nu_m}{4}\|\nabla w_h^{n+1}\|^2 + \frac{(\nu-\nu_m)^2}{4(\nu+\nu_m)}\|\nabla v_h^n\|^2 \\
&\qquad + \|f_1(t^{n+1})\|_{-1}\|\nabla v_h^{n+1}\| + \|f_2(t^{n+1})\|_{-1}\|\nabla w_h^{n+1}\|.
\end{aligned}$$

Reducing and dropping the non-negative terms $\|v_h^{n+1}-v_h^n\|^2$, $\|w_h^{n+1}-w_h^n\|^2$ on the left hand side gives us

$$\begin{aligned}\frac{1}{2\Delta t}&\left(\|v_h^{n+1}\|^2-\|v_h^n\|^2+\|w_h^{n+1}\|^2-\|w_h^n\|^2\right)\\&+\frac{\nu+\nu_m}{4}\left(\|\nabla v_h^{n+1}\|^2-\frac{(\nu-\nu_m)^2}{(\nu+\nu_m)^2}\|\nabla v_h^n\|^2\right)\\&+\frac{\nu+\nu_m}{4}\left(\|\nabla w_h^{n+1}\|^2-\frac{(\nu-\nu_m)^2}{(\nu+\nu_m)^2}\|\nabla w_h^n\|^2\right)\\&\leq\|f_1(t^{n+1})\|_{-1}\|\nabla v_h^{n+1}\|+\|f_2(t^{n+1})\|_{-1}\|\nabla w_h^{n+1}\|.\end{aligned}\tag{23}$$

Applying again Young's inequality with $\epsilon=\frac{\nu\nu_m}{\nu+\nu_m}$, we have

$$\begin{aligned}\frac{1}{2\Delta t}&\left(\|v_h^{n+1}\|^2-\|v_h^n\|^2+\|w_h^{n+1}\|^2-\|w_h^n\|^2\right)+\frac{\nu\nu_m}{2(\nu+\nu_m)}\|\nabla v_h^{n+1}\|^2\\&+\frac{(\nu-\nu_m)^2}{4(\nu+\nu_m)}\left(\|\nabla v_h^{n+1}\|^2-\|\nabla v_h^n\|^2\right)+\frac{\nu\nu_m}{2(\nu+\nu_m)}\|\nabla w_h^{n+1}\|^2\\&+\frac{(\nu-\nu_m)^2}{4(\nu+\nu_m)}\left(\|\nabla w_h^{n+1}\|^2-\|\nabla w_h^n\|^2\right)\\&\leq\frac{(\nu+\nu_m)}{2\nu\nu_m}\left(\|f_1(t^{n+1})\|_{-1}^2+\|f_2(t^{n+1})\|_{-1}^2\right).\end{aligned}\tag{24}$$

Multiplying both sides by $2\Delta t$ and summing over timesteps finishes the proof. □

The proposed algorithm also converges optimally in space in time, with assumed smoothness of the true solution.

Theorem 3.1. *Assume (v,w,p) solves (9)-(10) and satisfying*

$$\begin{aligned}v,w&\in L^\infty(0,T;H^m(\Omega)),\quad m=max\{2,k+1\},\\v_t,w_t&\in L^\infty(0,T;H^{k+1}(\Omega)),\\v_{tt},w_{tt}&\in L^\infty(0,T;L^2(\Omega)).\end{aligned}\tag{25}$$

Then the solution (v_h,w_h) to Algorithm 3.1 converges to the true solution: for any $\Delta t>0$,

(26)

$$\|v(T)-v_h^M\|+\|w(T)-w_h^M\|+\frac{\nu^2+\nu_m^2}{4(\nu+\nu_m)}\Delta t\left(\|\nabla(v(T)-v_h^M)\|+\|\nabla(w(T)-w_h^M)\|\right)$$
$$+\frac{\nu\nu_m}{2(\nu+\nu_m)}\left\{\Delta t\sum_{n=1}^{M-1}\left(\|\nabla(v(t^n)-v_h^n)\|^2+\|\nabla(w(t^n)-w_h^n)\|^2\right)\right\}^{\frac12}\leq C(h^k+\Delta t).$$

Proof. We begin by obtaining the error equations. Continuous variational formulation of (9)-(12) at the time level t^{n+1} is given

$$\begin{aligned}&\left(\frac{v(t^{n+1})-v(t^n)}{\Delta t},\chi_h\right)+(w(t^{n+1})\cdot\nabla v(t^{n+1}),\chi_h)\\&-(\tilde B_0(t^{n+1})\cdot\nabla v(t^{n+1}),\chi_h)+\frac{\nu+\nu_m}{2}(\nabla v(t^{n+1}),\nabla\chi_h)\\&+\frac{\nu-\nu_m}{2}(\nabla(w(t^{n+1})-w(t^n)),\nabla\chi_h)+\frac{\nu-\nu_m}{2}(\nabla w(t^n),\nabla\chi_h)\\&=-\left(v_t(t^{n+1})-\frac{v(t^{n+1})-v(t^n)}{\Delta t},\chi_h\right)+(f_1(t^{n+1}),\chi_h)\end{aligned}\tag{27}$$

and

$$\begin{aligned}
&\left(\frac{w(t^{n+1})-w(t^n)}{\Delta t}, l_h\right) + (v(t^{n+1})\cdot\nabla w(t^{n+1}), l_h)\\
&+ (\tilde{B}_0(t^{n+1})\cdot\nabla w(t^{n+1}), l_h) + \frac{\nu+\nu_m}{2}(\nabla w(t^{n+1}), \nabla l_h)\\
&+ \frac{\nu-\nu_m}{2}(\nabla(v(t^{n+1})-v(t^n)), \nabla l_h) + \frac{\nu-\nu_m}{2}(\nabla v(t^n), \nabla l_h)\\
&= -\left(w_t(t^{n+1}) - \frac{w(t^{n+1})-w(t^n)}{\Delta t}, l_h\right) + (f_2(t^{n+1}), l_h) \qquad (28)
\end{aligned}$$

for all $\chi_h, l_h \in V_h$. Denote the errors by $e_v^{n+1} := v(t^{n+1}) - v_h^{n+1}$ and $e_w^{n+1} := w(t^{n+1}) - w_h^{n+1}$ for all $n = 0, 1, ..., M-1$. Subtracting (27) and (28) from (18) and (19), respectively, produces

$$\begin{aligned}
&\left(\frac{e_v^{n+1}-e_v^n}{\Delta t}, \chi_h\right) + \frac{\nu+\nu_m}{2}(\nabla e_v^{n+1}, \nabla\chi_h) + \frac{\nu-\nu_m}{2}(\nabla e_w^n, \nabla\chi_h)\\
&- (\tilde{B}_0(t^{n+1})\cdot\nabla e_v^{n+1}, \chi_h) + (e_w^n\cdot\nabla v(t^{n+1}), \chi_h) + (w_h^n\cdot\nabla e_v^{n+1}, \chi_h)\\
&= -G_1(t, v, w, \chi_h) \qquad (29)
\end{aligned}$$

and

$$\begin{aligned}
&\left(\frac{e_w^{n+1}-e_w^n}{\Delta t}, l_h\right) + \frac{\nu+\nu_m}{2}(\nabla e_w^{n+1}, \nabla l_h) + \frac{\nu-\nu_m}{2}(\nabla e_v^n, \nabla l_h)\\
&+ (\tilde{B}_0(t^{n+1})\cdot\nabla e_w^{n+1}, l_h) + (e_v^n\cdot\nabla w(t^{n+1}), l_h) + (v_h^n\cdot\nabla e_w^{n+1}, l_h)\\
&= -G_2(t, v, w, l_h), \qquad (30)
\end{aligned}$$

here

$$\begin{aligned}
G_1(t, v, w, \chi_h) :=& \left(v_t(t^{n+1}) - \frac{v(t^{n+1})+v(t^n)}{\Delta t}, \chi_h\right)\\
&+ ((w(t^{n+1})-w(t^n))\cdot\nabla v(t^{n+1}), \chi_h)\\
&+ \frac{\nu-\nu_m}{2}(\nabla(w(t^{n+1})-w(t^n)), \nabla\chi_h)
\end{aligned}$$

and

$$\begin{aligned}
G_2(t, v, w, \chi_h) :=& \left(w_t(t^{n+1}) - \frac{w(t^{n+1})-w(t^n)}{\Delta t}, \chi_h\right)\\
&+ ((v(t^{n+1})-v(t^n))\cdot\nabla w(t^{n+1}), \chi_h)\\
&+ \frac{\nu-\nu_m}{2}(\nabla(v(t^{n+1})-v(t^n)), \nabla\chi_h).
\end{aligned}$$

Decompose the errors into the interpolation errors and approximations terms:

$$\begin{aligned}
e_v^{n+1} &:= v(t^{n+1}) - v_h^{n+1} = (v(t^{n+1}) - \tilde{v}^{n+1}) - (v_h^{n+1} - \tilde{v}^{n+1}) := \eta_v^{n+1} - \phi_h^{n+1},\\
e_w^{n+1} &:= w(t^{n+1}) - w_h^{n+1} = (w(t^{n+1}) - \tilde{w}^{n+1}) - (w_h^{n+1} - \tilde{w}^{n+1}) := \eta_w^{n+1} - \psi_h^{n+1},
\end{aligned}$$

take $\chi_h = \phi_h^{n+1}$ and $\chi_h = \psi_h^{n+1}$, use the polarization identity $2(a-b, a) = \|a\|^2 - \|b\|^2 + \|a-b\|^2$, and noting that

$$\begin{aligned}
(\tilde{B}_0(t^{n+1})\cdot\nabla\phi_h^{n+1}, \phi_h^{n+1}) &= (\tilde{B}_0(t^{n+1})\cdot\nabla\psi_h^{n+1}, \psi_h^{n+1}) = 0,\\
(w_h^n\cdot\nabla\phi_h^{n+1}, \phi_h^{n+1}) &= (v_h^n\cdot\nabla\psi_h^{n+1}, \psi_h^{n+1}) = 0,
\end{aligned}$$

we then have

$$\frac{1}{2\Delta t}\left(\|\phi_h^{n+1}\|^2-\|\phi_h^n\|^2+\|\phi_h^{n+1}-\phi_h^n\|^2\right)+\frac{\nu+\nu_m}{2}\|\nabla\phi_h^{n+1}\|^2$$
$$\leq\left|\frac{1}{\Delta t}(\eta_v^{n+1}-\eta_v^n,\phi_h^{n+1})\right|+\frac{\nu+\nu_m}{2}|(\nabla\eta_v^{n+1},\nabla\phi_h^{n+1})|$$
$$+\frac{|\nu-\nu_m|}{2}|(\nabla\eta_w^n,\nabla\phi_h^{n+1})|+\frac{|\nu-\nu_m|}{2}|(\nabla\psi_h^n,\nabla\phi_h^{n+1})|$$
$$+|(\tilde{B}_0(t^{n+1})\cdot\nabla\eta_v^{n+1},\phi_h^{n+1})|+|(w_h^n\cdot\nabla\eta_v^{n+1},\phi_h^{n+1})|$$
$$+|(\eta_w^n\cdot\nabla v(t^{n+1}),\phi_h^{n+1})|+|(\psi_h^n\cdot\nabla v(t^{n+1}),\phi_h^{n+1})|+|G_1(t,v,w,\phi_h^{n+1})| \tag{31}$$

and

$$\frac{1}{2\Delta t}\left(\|\psi_h^{n+1}\|^2-\|\psi_h^n\|^2+\|\psi_h^{n+1}-\psi_h^n\|^2\right)+\frac{\nu+\nu_m}{2}\|\nabla\psi_h^{n+1}\|^2$$
$$\leq\frac{1}{\Delta t}\left|(\eta_w^{n+1}-\eta_w^n,\psi_h^{n+1})\right|+\frac{\nu+\nu_m}{2}|(\nabla\eta_w^{n+1},\nabla\psi_h^{n+1})|$$
$$+\frac{|\nu-\nu_m|}{2}|(\nabla\eta_v^n,\nabla\psi_h^{n+1})|+\frac{|\nu-\nu_m|}{2}|(\nabla\phi_h^n,\nabla\psi_h^{n+1})|$$
$$+|(\tilde{B}_0(t^{n+1})\cdot\nabla\eta_w^{n+1},\psi_h^{n+1})|+|(v_h^n\cdot\nabla\eta_w^{n+1},\psi_h^{n+1})|$$
$$+|(\eta_v^n\cdot\nabla w(t^{n+1}),\psi_h^{n+1})|+|(\phi_h^n\cdot\nabla w(t^{n+1}),\psi_h^{n+1})|+|G_2(t,v,w,\psi_h^{n+1})|. \tag{32}$$

We now find bounds on the right hand side terms of (31) only, since the estimates are similar for (32). Applying Cauchy-Schwarz and Young inequalities on the first four terms results in

$$\frac{1}{\Delta t}\left|(\eta_v^{n+1}-\eta_v^n,\phi_h^{n+1})\right|\leq\frac{\nu\nu_m}{16(\nu+\nu_m)}\|\nabla\phi_h^{n+1}\|^2+\frac{C(\nu+\nu_m)}{\nu\nu_m(\Delta t)}\int_{t^n}^{t^{n+1}}\|\partial_t\eta_v\|^2d\tau,$$
$$\frac{\nu+\nu_m}{2}|(\nabla\eta_v^{n+1},\nabla\phi_h^{n+1})|\leq\frac{\nu\nu_m}{16(\nu+\nu_m)}\|\nabla\phi_h^{n+1}\|^2+\frac{(\nu+\nu_m)^3}{\nu\nu_m}\|\nabla\eta_v^{n+1}\|^2,$$
$$\frac{|\nu-\nu_m|}{2}|(\nabla\eta_w^n,\nabla\phi_h^{n+1})|\leq\frac{\nu\nu_m}{16(\nu+\nu_m)}\|\nabla\phi_h^{n+1}\|^2+\frac{(\nu-\nu_m)^2(\nu+\nu_m)}{\nu\nu_m}\|\nabla\eta_w^n\|^2,$$
$$\frac{|\nu-\nu_m|}{2}|(\nabla\psi_h^n,\nabla\phi_h^{n+1})|\leq\frac{\nu+\nu_m}{4}\|\nabla\phi_h^{n+1}\|^2+\frac{(\nu-\nu_m)^2}{4(\nu+\nu_m)}\|\nabla\psi_h^n\|^2.$$

Applying Hölder and Young's inequalities with (13) on the first three nonlinear terms yields

$$|(\tilde{B}_0(t^{n+1})\cdot\nabla\eta_v^{n+1},\phi_h^{n+1})|$$
$$\leq C\|\tilde{B}_0(t^{n+1})\|_\infty\|\nabla\eta_v^{n+1}\|\|\nabla\phi_h^{n+1}\|$$
$$\leq\frac{\nu\nu_m}{16(\nu+\nu_m)}\|\nabla\phi_h^{n+1}\|^2+\frac{C(\nu+\nu_m)}{\nu\nu_m}\|\tilde{B}_0(t^{n+1})\|_\infty^2\|\nabla\eta_v^{n+1}\|^2,$$
$$|(w_h^n\cdot\nabla\eta_v^{n+1},\phi_h^{n+1})|\leq C\|\nabla w_h^n\|\|\nabla\eta_v^{n+1}\|\|\nabla\phi_h^{n+1}\|$$
$$\leq\frac{\nu\nu_m}{16(\nu+\nu_m)}\|\nabla\phi_h^{n+1}\|^2+\frac{C(\nu+\nu_m)}{\nu\nu_m}\|\nabla w_h^n\|^2\|\nabla\eta_v^{n+1}\|^2,$$
$$|(\eta_w^n\cdot\nabla v(t^{n+1}),\phi_h^{n+1})|\leq C\|\nabla\eta_w^n\|\|\nabla v(t^{n+1})\|\|\nabla\phi_h^{n+1}\|$$
$$\leq\frac{\nu\nu_m}{16(\nu+\nu_m)}\|\nabla\phi_h^{n+1}\|^2+\frac{C(\nu+\nu_m)}{\nu\nu_m}\|\nabla v(t^{n+1})\|^2\|\nabla\eta_w^n\|^2.$$

For the last nonlinear term, we use Hölder's inequality, Sobolev embedding theorems, Poincare's and Young's inequalities to reveal

$$
\begin{aligned}
|(\psi_h^n \cdot \nabla v(t^{n+1}), \phi_h^{n+1})| &\le C\|\psi_h^n\|\nabla v(t^{n+1})\|_{L^6}\|\phi_h^{n+1}\|_{L^3} \\
&\le C\|\psi_h^n\|\|v(t^{n+1})\|_{H^2}\|\phi_h^n\|^{1/2}\|\nabla\phi_h^{n+1}\|^{1/2} \\
&\le C\|\psi_h^n\|\|v(t^{n+1})\|_{H^2}\|\nabla\phi_h^{n+1}\| \\
&\le \frac{\nu\nu_m}{16(\nu+\nu_m)}\|\nabla\phi_h^{n+1}\|^2 + \frac{C(\nu+\nu_m)}{\nu\nu_m}\|v(t^{n+1})\|_{H^2}^2\|\psi_h^n\|^2.
\end{aligned}
$$

The last term is evaluated as in [20]:

$$
\begin{aligned}
|G_1(t,v,w,\phi_h^{n+1})| \le{}& \frac{\nu\nu_m}{16(\nu+\nu_m)}\|\nabla\phi_h^{n+1}\|^2 + \frac{(\Delta t)^2(\nu+\nu_m)}{\nu\nu_m} \\
&\times\left(C\|v_{tt}(t^{**})\|^2 + \frac{(\nu-\nu_m)^2}{4}\|\nabla w_t(s^*)\|^2 + C\|\nabla w_t(s^*)\|^2\|\nabla v(t^{n+1})\|^2\right)
\end{aligned}
$$

with $t^{**}, s^* \in [t^n, t^{n+1}]$. Putting these estimates into (31) and dropping non-negative term on the left hand side produces

$$
\begin{aligned}
&\frac{1}{2\Delta t}\left(\|\phi_h^{n+1}\|^2 - \|\phi_h^n\|^2\right) + \frac{\nu^2+\nu_m^2}{4(\nu+\nu_m)}\|\nabla\phi_h^{n+1}\|^2 \\
\le{}& \frac{(\nu-\nu_m)^2}{4(\nu+\nu_m)}\|\nabla\psi_h^n\|^2 + \frac{C(\nu+\nu_m)}{\nu\nu_m}\|v(t^{n+1})\|_{H^2}^2\|\psi_h^n\|^2 \\
&+ \frac{C(\nu+\nu_m)}{\nu\nu_m(\Delta t)}\int_{t^n}^{t^{n+1}}\|\partial_t\eta_v\|^2 d\tau + \frac{(\nu+\nu_m)^3}{\nu\nu_m}\|\nabla\eta_v^{n+1}\|^2 \\
&+ \frac{(\nu-\nu_m)^2(\nu+\nu_m)}{\nu\nu_m}\|\nabla\eta_w^n\|^2 \\
&+ \frac{C(\nu+\nu_m)}{\nu\nu_m}\left[\left(\|\tilde{B}_0(t^{n+1})\|_\infty^2 + \|\nabla w_h^n\|^2\right)\|\nabla\eta_v^{n+1}\|^2\right. \\
&\left.+ \|\nabla v(t^{n+1})\|^2\|\nabla\eta_w^n\|^2\right] + \frac{(\Delta t)^2(\nu+\nu_m)}{\nu\nu_m}\left(C\|v_{tt}(t^{**})\|^2\right. \\
&\left.+ \frac{(\nu-\nu_m)^2}{4}\|\nabla w_t(s^*)\|^2 + C\|\nabla w_t(s^*)\|^2\|\nabla v(t^{n+1})\|^2\right).
\end{aligned}
\tag{33}
$$

Applying similar techniques to (32), we get

$$
\begin{aligned}
&\frac{1}{2\Delta t}\left(\|\psi_h^{n+1}\|^2 - \|\psi_h^n\|^2\right) + \frac{\nu^2+\nu_m^2}{4(\nu+\nu_m)}\|\nabla\psi_h^{n+1}\|^2 \\
\le{}& \frac{C(\nu+\nu_m)}{\nu\nu_m(\Delta t)}\int_{t^n}^{t^{n+1}}\|\partial_t\eta_w\|^2 d\tau + \frac{C(\nu+\nu_m)}{\nu\nu_m}\|w(t^{n+1})\|_{H^2}^2\|\phi_h^n\|^2 \\
&+ \frac{(\nu-\nu_m)^2}{4(\nu+\nu_m)}\|\nabla\phi_h^n\|^2 + \frac{(\nu+\nu_m)^3}{\nu\nu_m}\|\nabla\eta_w^{n+1}\|^2 + \frac{(\nu-\nu_m)^2(\nu+\nu_m)}{\nu\nu_m}\|\nabla\eta_v^n\|^2 \\
&+ \frac{C(\nu+\nu_m)}{\nu\nu_m}\left[\left(\|\tilde{B}_0(t^{n+1})\|_\infty^2 + \|\nabla v_h^n\|^2\right)\|\nabla\eta_w^{n+1}\|^2\right. \\
&\left.+ \|\nabla w(t^{n+1})\|^2\|\nabla\eta_v^n\|^2\right] + \frac{(\Delta t)^2(\nu+\nu_m)}{\nu\nu_m}\left(C\|w_{tt}(s^{**})\|^2\right. \\
&\left.+ \frac{(\nu-\nu_m)^2}{4}\|\nabla v_t(t^*)\|^2 + C\|\nabla v_t(t^*)\|^2\|\nabla w(t^{n+1})\|^2\right),
\end{aligned}
\tag{34}
$$

with $s^{**}, t^* \in [t^n, t^{n+1}]$.
Now add equations (33) and (34), multiply by $2\Delta t$ and sum over the time steps. Using interpolation properties (15)-(16) with noting that $\|\psi_h^0\| = \|\phi_h^0\| = 0$ and $\Delta t M = T$ yields

$$
\begin{aligned}
(35) \qquad & \Big(\|\phi_h^M\|^2 + \|\psi_h^M\|^2\Big) + \frac{\nu^2+\nu_m^2}{4(\nu+\nu_m)}(\|\nabla\phi_h^M\|^2 \\
& + \|\nabla\psi_h^M\|^2) + \frac{\nu\nu_m}{2(\nu+\nu_m)}\Delta t\sum_{n=0}^{M-2}(\|\nabla\phi_h^{n+1}\|^2 + \|\nabla\psi_h^{n+1}\|^2) \\
\leq & \Delta t\sum_{n=0}^{M-1} C\frac{(\nu+\nu_m)}{\nu\nu_m}\Big(\|w\|^2_{L^\infty(0,T;H^2(\Omega))}\|\phi_h^n\|^2 + \|v\|^2_{L^\infty(0,T;H^2(\Omega))}\|\psi_h^n\|^2\Big) \\
& + \frac{C(\nu+\nu_m)}{\nu\nu_m}\int_0^T\Big(\|\partial_t\eta_v\|^2 + \|\partial_t\eta_w\|^2\Big)d\tau \\
& + C^*h^{2k}\Delta t\sum_{n=0}^{M-1}\Big(|v(t^{n+1})|^2_{k+1} + |w(t^{n+1})|^2_{k+1}\Big) \\
& + C^*h^{2k}\Delta t\sum_{n=0}^{M-1}\Big(|v(t^n)|^2_{k+1} + |w(t^n)|^2_{k+1}\Big) + C^*(\Delta t)^2 \\
& + C^*h^{2k}\Delta t\sum_{n=0}^{M-1}\Big(\|\nabla v_h^n\|^2|w(t^{n+1})|^2_{k+1} + \|\nabla w_h^n\|^2|v(t^{n+1})|^2_{k+1}\Big),
\end{aligned}
$$

where $C^* := C^*(C, T, \nu, \nu_m, v, w, \tilde{B}_0(t))$ and it is independent of the time step Δt and h. Using smoothness assumptions, approximation properties (15)-(16), and the stability bounds on the discrete solutions in (35) gives

$$
\begin{aligned}
& \Big(\|\phi_h^M\|^2 + \|\psi_h^M\|^2\Big) \\
& + \frac{\nu^2+\nu_m^2}{4(\nu+\nu_m)}(\|\nabla\phi_h^M\|^2 + \|\nabla\psi_h^M\|^2) + \frac{\nu\nu_m}{2(\nu+\nu_m)}\Delta t\sum_{n=0}^{M-2}(\|\nabla\phi_h^{n+1}\|^2 + \|\nabla\psi_h^{n+1}\|^2) \\
& \leq \Delta t\sum_{n=0}^{M-1} C^*\Big(\|\phi_h^n\|^2 + \|\psi_h^n\|^2\Big) + C^*(\Delta t)^2 + C^*(h^{2k} + h^{2k+2}).
\end{aligned}
$$

The result follows from application of the discrete Gronwall lemma and the triangle inequality. We note that since there is no $\|\phi_h^M\|^2$ or $\|\psi_h^M\|^2$ on the right hand side (the sum ends at M-1) there is no timestep restriction for the application of the Gronwall lemma.

□

4. Penalty-projection method for MHD in Elsässer Variables

The algorithm studied in the previous section decouples into 2 sub-problems at each timestep, each of which takes the form of an Oseen problem. It is known that splitting methods such as the penalty-projection method can more efficiently give solutions to such problems, with often very little sacrifice in accuracy [1, 18, 21]. We therefore propose in this section a scheme that uses penalty-projection methods for the 2 sub-problems. Because of the splitting, it is necessary to define an additional velocity space: $Y_h = (P_k)^d \cap H_0^{div}(\Omega)^d$. The only difference between Y_h and X_h is simply that the boundary condition of Y_h is only enforced in the normal direction, while for X_h it is enforced in all directions.

The proposed scheme takes the following form.

Algorithm 4.1. *(Grad-div stabilized projection scheme):Let* $f_1, f_2 \in L^\infty(0,T;H^{-1}(\Omega))$, *stabilization parameter* $\gamma > 0$ *and time step* $\Delta t > 0$ *and end time* $T > 0$ *be given. Set* $M = T/\Delta t$ *and start with* $\tilde{v}^0 = v(0), \tilde{w}^0 = w(0) \in H^2 \cup V$. *For all* $n = 0,1,...,M-1$, *compute* $\hat{v}_h^{n+1}, \hat{w}_h^{n+1}, \hat{p}_h^{n+1}, \hat{q}_h^{n+1}$ *via:*
Step 1: Find $\hat{v}^{n+1} \in X_h$ *satisfying for all* $\chi_h \in X_h$,

$$\begin{aligned}\left(\frac{\hat{v}_h^{n+1}-\tilde{v}_h^n}{\Delta t},\chi_h\right) &+ b^*(\hat{w}_h^n,\hat{v}_h^{n+1},\chi_h) - (\tilde{B}_0(t^{n+1})\cdot\nabla\hat{v}_h^{n+1},\chi_h)\\ &+\frac{\nu+\nu_m}{2}(\nabla\hat{v}_h^{n+1},\nabla\chi_h)+\frac{\nu-\nu_m}{2}(\nabla\hat{w}_h^n,\nabla\chi_h)\\ &+\gamma(\nabla\cdot\hat{v}_h^{n+1},\nabla\cdot\chi_h) = (f_1(t^{n+1}),\chi_h).\end{aligned} \tag{36}$$

Step 2: Find $(\tilde{v}_h^{n+1}, \hat{q}_h^{n+1}) \in (Y_h \times Q_h)$ *satisfying for all* $(v_h, q_h) \in (Y_h \times Q_h)$,

$$\left(\frac{\tilde{v}_h^{n+1}-\hat{v}_h^{n+1}}{\Delta t},v_h\right) - (\hat{q}_h^{n+1},\nabla\cdot v_h) = 0, \tag{37}$$

$$(\nabla\cdot\tilde{v}^{n+1},q_h) = 0. \tag{38}$$

Step 3: Compute $\hat{w}_h^{n+1} \in X_h$ *for all* $l_h \in X_h$,

$$\begin{aligned}\left(\frac{\hat{w}_h^{n+1}-\tilde{w}_h^n}{\Delta t},l_h\right) &+ b^*(\hat{v}_h^n,\hat{w}_h^{n+1},l_h) + (\tilde{B}_0(t^{n+1})\cdot\nabla\hat{w}_h^{n+1},l_h) + \frac{\nu+\nu_m}{2}(\nabla\hat{w}_h^{n+1},\nabla l_h)\\ &+\frac{\nu-\nu_m}{2}(\nabla\hat{v}_h^n,\nabla l_h)+\gamma(\nabla\cdot\hat{w}_h^{n+1},\nabla\cdot l_h) = (f_2(t^{n+1}),l_h).\end{aligned} \tag{39}$$

Step 4: Find $(\tilde{w}_h^{n+1}, \hat{\lambda}_h^{n+1}) \in (Y_h \times Q_h)$ *satisfying for all* $(s_h, r_h) \in (Y_h \times Q_h)$,

$$\left(\frac{\tilde{w}_h^{n+1}-\hat{w}_h^{n+1}}{\Delta t},s_h\right) - (\hat{\lambda}_h^{n+1},\nabla\cdot s_h) = 0, \tag{40}$$

$$(\nabla\cdot\tilde{w}_h^{n+1},r_h) = 0. \tag{41}$$

Since $X_h \subset Y_h$, we can choose $v_h = \chi_h$ in (37), $s_h = l_h$ in (40) and combine these with equations (36) and (39), respectively, to get

$$\begin{aligned}\left(\tfrac{\hat{v}_h^{n+1}-\hat{v}_h^n}{\Delta t},\chi_h\right) &+ b^*(\hat{w}_h^n,\hat{v}_h^{n+1},\chi_h) - (\tilde{B}_0(t^{n+1})\cdot\nabla\hat{v}_h^{n+1},\chi_h)\\ +\tfrac{\nu+\nu_m}{2}(\nabla\hat{v}_h^{n+1},\nabla\chi_h) &+ \tfrac{\nu-\nu_m}{2}(\nabla\hat{w}_h^n,\nabla\chi_h)+\gamma(\nabla\cdot\hat{v}_h^{n+1},\nabla\cdot\chi_h)\\ &-(\hat{q}_h^n,\nabla\cdot\chi_h) = (f_1(t^{n+1}),\chi_h).\end{aligned} \tag{42}$$

and

$$\begin{aligned}&\left(\frac{\hat{w}_h^{n+1}-\hat{w}_h^n}{\Delta t},l_h\right) + b^*(\hat{v}_h^n,\hat{w}_h^{n+1},l_h) + (\tilde{B}_0(t^{n+1})\cdot\nabla\hat{w}_h^{n+1},l_h)\\ &+\frac{\nu+\nu_m}{2}(\nabla\hat{w}_h^{n+1},\nabla l_h)+\frac{\nu-\nu_m}{2}(\nabla\hat{v}_h^n,\nabla l_h)+\gamma(\nabla\cdot\hat{w}_h^{n+1},\nabla\cdot l_h)\\ &-(\hat{\lambda}_h^n,\nabla\cdot l_h) = (f_2(t^{n+1}),l_h).\end{aligned} \tag{43}$$

We first prove unconditional stability of the penalty-projection scheme.

Lemma 4.1. *(Unconditional Stability) Let* $(\hat{v}_h^{n+1}, \hat{w}_h^{n+1}, \hat{q}_h^{n+1}, \hat{\lambda}_h^{n+1})$ *be the solution of Algorithm 4.1 and* $f_1, f_2 \in L^\infty(0,T; H^{-1}(\Omega))$*. Then for all* $\Delta t > 0$*, we have the following unconditional stability bound:*

$$\begin{aligned}(44)\quad & \|\hat{v}_h^M\|^2 + \|\hat{w}_h^M\|^2 + \frac{(\nu-\nu_m)^2}{2(\nu+\nu_m)}\Delta t(\|\nabla \hat{v}_h^M\|^2 + \|\nabla \hat{w}_h^M\|^2) \\ & + \frac{\nu\nu_m}{\nu+\nu_m}\Delta t \sum_{n=0}^{M-1}\left(\|\nabla \hat{v}_h^{n+1}\|^2 + \|\nabla \hat{w}_h^{n+1}\|^2\right) + \Delta t \sum_{n=0}^{M-1}\gamma(\|\nabla\cdot \hat{v}_h^{n+1}\|^2 + \|\nabla\cdot \hat{w}_h^{n+1}\|^2) \\ & \leq \|\hat{v}_h^0\|^2 + \|\hat{w}_h^0\|^2 + \frac{(\nu-\nu_m)^2}{2(\nu+\nu_m)}\Delta t(\|\nabla \hat{v}_h^0\|^2 + \|\nabla \hat{w}_h^0\|^2) \\ & \qquad + \frac{\nu+\nu_m}{\nu\nu_m}\Delta t \sum_{n=0}^{M-1}(\|f_1(t^{n+1})\|_{-1}^2 + \|f_2(t^{n+1})\|_{-1}^2)\end{aligned}$$

Proof. Taking $\chi_h = \hat{v}_h^{n+1}$ in (36) and $l_h = \hat{w}_h^{n+1}$ in (39) with the polarization identity produces

$$\begin{aligned}& \frac{1}{2\Delta t}(\|\hat{v}_h^{n+1}\|^2 - \|\tilde{v}_h^n\|^2 + \|\hat{v}_h^{n+1} - \tilde{v}_h^n\|^2) + \frac{\nu+\nu_m}{2}\|\nabla \hat{v}_h^{n+1}\|^2 + \gamma\|\nabla\cdot \hat{v}_h^{n+1}\|^2 \\ (45)\quad & \qquad = -\frac{\nu-\nu_m}{2}(\nabla \hat{w}_h^n, \nabla \hat{v}_h^{n+1}) + (f_1(t^{n+1}), \hat{v}_h^{n+1})\end{aligned}$$

and

$$\begin{aligned}& \frac{1}{2\Delta t}(\|\hat{w}_h^{n+1}\|^2 - \|\tilde{w}_h^n\|^2 + \|\hat{w}_h^{n+1} - \tilde{w}_h^n\|^2) + \frac{\nu+\nu_m}{2}\|\nabla \hat{w}_h^{n+1}\|^2 + \gamma\|\nabla\cdot \hat{w}_h^{n+1}\|^2 \\ (46)\quad & \qquad = -\frac{\nu-\nu_m}{2}(\nabla \hat{v}_h^n, \nabla \hat{w}_h^{n+1}) + (f_2(t^{n+1}), \hat{w}_h^{n+1}).\end{aligned}$$

Applying Cauchy-Schwarz and Young's inequalities on the right hand sides terms of (45) and (46) gives

$$\begin{aligned}\frac{|\nu-\nu_m|}{2}|(\nabla \hat{w}_h^n, \nabla \hat{v}_h^{n+1})| &\leq \frac{\nu+\nu_m}{4}\|\nabla \hat{v}_h^{n+1}\|^2 + \frac{(\nu-\nu_m)^2}{4(\nu+\nu_m)}\|\nabla \hat{w}_h^n\|^2, \\ |(f_1(t^{n+1}), \hat{v}_h^{n+1})| &\leq \frac{\nu\nu_m}{2(\nu+\nu_m)}\|\nabla \hat{v}_h^{n+1}\|^2 + \frac{(\nu+\nu_m)}{2(\nu\nu_m)}\|f_1(t^{n+1})\|_{-1}^2, \\ \frac{|\nu-\nu_m|}{2}|(\nabla \hat{v}_h^n, \nabla \hat{w}_h^{n+1})| &\leq \frac{\nu+\nu_m}{4}\|\nabla \hat{w}_h^{n+1}\|^2 + \frac{(\nu-\nu_m)^2}{4(\nu+\nu_m)}\|\nabla \hat{v}_h^n\|^2, \\ |(f_2(t^{n+1}), \hat{w}_h^{n+1})| &\leq \frac{\nu\nu_m}{2(\nu+\nu_m)}\|\nabla \hat{w}_h^{n+1}\|^2 + \frac{(\nu+\nu_m)}{2(\nu\nu_m)}\|f_2(t^{n+1})\|_{-1}^2.\end{aligned}$$

Now choose $v_h = \tilde{v}_h^{n+1}$ in (37), $q_h = \hat{q}_h^{n+1}$ in (38) and $s_h = \tilde{w}_h^{n+1}$ in (40), $r_h = \hat{\lambda}_h^{n+1}$ in (41). Then apply Cauchy-Schwarz and Young's inequalities to obtain

$$\begin{aligned}\|\tilde{v}_h^{n+1}\|^2 &\leq \|\hat{v}_h^{n+1}\|^2, \\ \|\tilde{w}_h^{n+1}\|^2 &\leq \|\hat{w}_h^{n+1}\|^2.\end{aligned}$$

for all $n = 0, 1, 2, ..., M-1$. Plugging these estimates into (45) and (46), dropping the non-negative terms results in

$$\begin{aligned}
&\frac{1}{2\Delta t}(\|\hat{v}_h^{n+1}\|^2 - \|\hat{v}_h^n\|^2) + \frac{(\nu-\nu_m)^2}{4(\nu+\nu_m)}\|\nabla\hat{v}_h^{n+1}\|^2 \\
&+ \frac{\nu\nu_m}{2(\nu+\nu_m)}\|\nabla\hat{v}_h^{n+1}\|^2 + \gamma\|\nabla\cdot\hat{v}_h^{n+1}\|^2 \\
&\leq \frac{(\nu-\nu_m)^2}{4(\nu+\nu_m)}\|\nabla\hat{w}_h^n\|^2 + \frac{\nu+\nu_m}{2\nu\nu_m}\|f_1(t^{n+1})\|_{-1}^2
\end{aligned} \tag{47}$$

and

$$\begin{aligned}
&\frac{1}{2\Delta t}(\|\hat{w}_h^{n+1}\|^2 - \|\hat{w}_h^n\|^2) + \frac{(\nu-\nu_m)^2}{4(\nu+\nu_m)}\|\nabla\hat{w}_h^{n+1}\|^2 + \frac{\nu\nu_m}{2(\nu+\nu_m)}\|\nabla\hat{w}_h^{n+1}\|^2 + \gamma\|\nabla\cdot\hat{w}_h^{n+1}\|^2 \\
&\leq \frac{(\nu-\nu_m)^2}{4(\nu+\nu_m)}\|\nabla\hat{v}_h^n\|^2 + \frac{\nu+\nu_m}{2\nu\nu_m}\|f_2(t^{n+1})\|_{-1}^2.
\end{aligned} \tag{48}$$

Adding these two equations, multiplying by $2\Delta t$ and summing over time steps finishes the proof. □

We now prove convergence of Algorithm 4.1 to Algorithm 3.1 as $\gamma \to \infty$. To do so, we will need to define the space $R_h := V_h^{\perp} \subset X_h$ to be the orthogonal complement of V_h with respect to the norm $H^1(\Omega)$. The following lemma gives the equivalence of the divergence and gradient norms in the space R_h, which is proven in [13] in a very general setting, and a simpler proof for the case of Scott-Vogelius elements is given in [21].

Lemma 4.2. *Let $(X_h, Q_h) \subset (X, Q)$ be finite element pairs satisfying the inf-sup condition (14) and the divergence-free property, i.e., $\nabla \cdot X_h \subset Q_h$. Then there exists a constant C_R independent of h such that*

$$\|\nabla v_h\| \leq C_R\|\nabla\cdot v_h\|, \quad \forall v_h \in R_h.$$

Assumption 4.1. *Let's assume that there exists a constant C_* which is independent of $h, \Delta t$ and γ, such that for sufficiently small h and Δt, the solutions of Algorithm 3.1 and Algorithm 4.1 satisfy*

$$\max_{1\leq n\leq M}(\|\nabla v_h^n\|_{L^3} + \|\nabla w_h^n\|_{L^3} + \|v_h^n\|_\infty + \|w_h^n\|_\infty) \leq C_*,$$
$$\max_{1\leq n\leq M}(\|\nabla\hat{v}_h^n\| + \|\nabla\hat{w}_h^n\|) \leq C_*.$$

Theorem 4.1. *Let $(v_h^{n+1}, w_h^{n+1}, q_h^{n+1})$ and $(\hat{v}_h^{n+1}, \hat{w}_h^{n+1}, \hat{q}_h^{n+1})$ be solutions of the Algorithm 3.1 and Algorithm 4.1, respectively, for $n = 0, 1, 2, ..., M-1$. We then have the following:*

$$\begin{aligned}
&\left(\Delta t \sum_{=0}^{M-1}\left(\|\nabla(v_h^{n+1} - \hat{v}_h^{n+1})\|^2 + \|\nabla(w_h^{n+1} - \hat{w}_h^{n+1})\|^2\right)\right)^{\frac{1}{2}} \\
&\leq \gamma^{-1}C\max\{C_*(\frac{\nu+\nu_m}{\nu\nu_m})^{1/2}, (\Delta t)^{-1/2}\}\left(\Delta t\sum_{n=0}^{M-1}\left(\|q_h^{n+1} - \hat{q}_h^n\|^2 + \|\lambda_h^{n+1} - \hat{\lambda}_h^n\|^2\right)\right)^{\frac{1}{2}}.
\end{aligned}$$

Remark 4.1. *The theorem shows that on a fixed mesh and timestep, penalty-projection solutions have first order convergence to the Algorithm 3.1 solution as $\gamma \to \infty$. This shows that for large penalty parameters, we can use the penalty-projection method and get the same accuracy as Algorithm 3.1.*

Proof. Denote $e^{n+1} := v_h^{n+1} - \hat{v}_h^{n+1}$ and $\epsilon^{n+1} := w_h^{n+1} - \hat{w}_h^{n+1}$ and decompose the errors orthogonally as follows:

$$e^{n+1} := e_0^{n+1} + e_R^{n+1},\ \epsilon^{n+1} := \epsilon_0^{n+1} + \epsilon_R^{n+1}$$

with $e_0^{n+1}, \epsilon_0^{n+1} \in V_h$ and $e_R^{n+1}, \epsilon_R^{n+1} \in R_h$, $n = 0, 1, ..., M-1$.
Step 1: *Estimate of* $e_R^{n+1}, \epsilon_R^{n+1}$*:*
Subtracting the equation (18) from (42) and (19) from (43) produces

$$\begin{aligned}
&\frac{1}{\Delta t}\left(e^{n+1} - e^n, \chi_h\right) + \frac{\nu + \nu_m}{2}(\nabla e^{n+1}, \nabla \chi_h) \\
&+ \gamma(\nabla \cdot e_R^{n+1}, \nabla \cdot \chi_h) + \frac{\nu - \nu_m}{2}(\nabla \epsilon^n, \nabla \chi_h) \\
&- (\tilde{B}_0(t^{n+1}) \cdot \nabla e^{n+1}, \chi_h) + b^*(\epsilon^n, v_h^{n+1}, \chi_h) \\
&+ b^*(\hat{w}_h^n, e^{n+1}, \chi_h) - (q_h^{n+1} - \hat{q}_h^n, \nabla \cdot \chi_h) = 0,
\end{aligned} \tag{49}$$

and

$$\begin{aligned}
&\frac{1}{\Delta t}\left(\epsilon^{n+1} - \epsilon^n, l_h\right) + \frac{\nu + \nu_m}{2}(\nabla \epsilon^{n+1}, \nabla l_h) + \gamma(\nabla \cdot \epsilon_R^{n+1}, \nabla \cdot l_h) \\
&+ \frac{\nu - \nu_m}{2}(\nabla e^n, \nabla l_h) + (\tilde{B}_0(t^{n+1}) \cdot \nabla \epsilon^{n+1}, l_h) + b^*(e^n, w_h^{n+1}, l_h) \\
&+ b^*(\hat{v}_h^n, \epsilon^{n+1}, l_h) - (\lambda_h^{n+1} - \hat{\lambda}_h^n, \nabla \cdot l_h) = 0.
\end{aligned} \tag{50}$$

Take $\chi_h = e^{n+1}$ in (49), $l_h = \epsilon^{n+1}$ in (50), which yield

$$\begin{aligned}
b^*(\hat{w}_h^n, e^{n+1}, e^{n+1}) = (\tilde{B}_0(t^{n+1}) \cdot \nabla e^{n+1}, e^{n+1}) = 0 \\
b^*(\hat{v}_h^n, \epsilon^{n+1}, \epsilon^{n+1}) = (\tilde{B}_0(t^{n+1}) \cdot \nabla \epsilon^{n+1}, \epsilon^{n+1}) = 0
\end{aligned}$$

and use polarization identity $2(a-b, a) = \|a\|^2 - \|b\|^2 + \|a-b\|^2$ to get

$$\begin{aligned}
&\frac{1}{2\Delta t}\left(\|e^{n+1}\|^2 - \|e^n\|^2 + \|e^{n+1} - e^n\|^2\right) + \frac{\nu + \nu_m}{2}\|\nabla e^{n+1}\|^2 + \gamma\|\nabla \cdot e_R^{n+1}\|^2 \\
&\quad = -\frac{\nu - \nu_m}{2}(\nabla \epsilon^n, \nabla e^{n+1}) + (q_h^{n+1} - \hat{q}_h^n, \nabla \cdot e_R^{n+1}) - b^*(\epsilon^n, v_h^{n+1}, e^{n+1})
\end{aligned} \tag{51}$$

and

$$\begin{aligned}
&\frac{1}{2\Delta t}\left(\|\epsilon^{n+1}\|^2 - \|\epsilon^n\|^2 + \|\epsilon^{n+1} - \epsilon^n\|^2\right) + \frac{\nu + \nu_m}{2}\|\nabla \epsilon^{n+1}\|^2 + \gamma\|\nabla \cdot \epsilon_R^{n+1}\|^2 \\
&\quad = -\frac{\nu - \nu_m}{2}(\nabla e^n, \nabla \epsilon^{n+1}) + (\lambda_h^{n+1} - \hat{\lambda}_h^n, \nabla \cdot \epsilon_R^{n+1}) - b^*(e^n, w_h^{n+1}, \epsilon^{n+1}).
\end{aligned} \tag{52}$$

Applying Cauchy-Schwarz and Young's inequalities to the first two terms of (51) provides

$$\begin{aligned}
\frac{|\nu - \nu_m|}{2}|(\nabla \epsilon^n, \nabla e^{n+1})| &\le \frac{(\nu - \nu_m)^2}{4(\nu + \nu_m)}\|\nabla \epsilon^n\|^2 + \frac{\nu + \nu_m}{4}\|\nabla e^{n+1}\|^2, \\
(q_h^{n+1} - \hat{q}_h^n, \nabla \cdot e_R^{n+1}) &\le \frac{\gamma^{-1}}{2}\|q_h^{n+1} - \hat{q}_h^n\|^2 + \frac{\gamma}{2}\|\nabla \cdot e_R^{n+1}\|^2.
\end{aligned}$$

and using Hölder's and Young's inequalities with Sobolev embedding theorem along with Assumption 4.1 on the non-linear term yields:

$$
\begin{aligned}
|b^*(\epsilon^n, v_h^{n+1}, e^{n+1})| &\leq C\Big(\|\epsilon^n\|\|\nabla v_h^{n+1}\|_{L^3}\|\nabla e^{n+1}\| + \|\epsilon^n\|\|v_h^{n+1}\|_{L^\infty}\|\nabla e^{n+1}\|\Big) \\
&\leq CC_*\|\epsilon^n\|\|\nabla e^{n+1}\| \\
&\leq \frac{\nu\nu_m}{2(\nu+\nu_m)}\|\nabla e^{n+1}\|^2 + \frac{CC_*^2(\nu+\nu_m)}{\nu\nu_m}\|\epsilon^n\|^2.
\end{aligned}
$$

Substituting these estimates in (51), adding and subtracting the term $\frac{\nu\nu_m}{2(\nu+\nu_m)}\|\nabla e^{n+1}\|^2$ with dropping the non-negative term $\|e^{n+1}-e^n\|^2$ gives us

$$
\begin{aligned}
&\frac{1}{2\Delta t}(\|e^{n+1}\|^2 - \|e^n\|^2) + \frac{(\nu-\nu_m)^2}{4(\nu+\nu_m)}\|\nabla e^{n+1}\|^2 + \frac{\nu\nu_m}{2(\nu+\nu_m)}\|\nabla e^{n+1}\|^2 + \frac{\gamma}{2}\|\nabla\cdot e_R^{n+1}\|^2 \\
&\leq \frac{(\nu-\nu_m)^2}{4(\nu+\nu_m)}\|\nabla \epsilon^n\|^2 + \frac{CC_*^2(\nu+\nu_m)}{\nu\nu_m}\|\epsilon^n\|^2 + \frac{\gamma^{-1}}{2}\|q_h^{n+1} - \hat{q}_h^n\|^2. \qquad (53)
\end{aligned}
$$

Now apply similar estimates to the right hand side terms of (52) to produce

$$
\begin{aligned}
&\frac{1}{2\Delta t}(\|\epsilon^{n+1}\|^2 - \|\epsilon^n\|^2) + \frac{(\nu-\nu_m)^2}{4(\nu+\nu_m)}\|\nabla \epsilon^{n+1}\|^2 + \frac{\nu\nu_m}{2(\nu+\nu_m)}\|\nabla \epsilon^{n+1}\|^2 + \frac{\gamma}{2}\|\nabla\cdot \epsilon_R^{n+1}\|^2 \\
&\leq \frac{(\nu-\nu_m)^2}{4(\nu+\nu_m)}\|\nabla e^n\|^2 + \frac{CC_*^2(\nu+\nu_m)}{\nu\nu_m}\|e^n\|^2 + \frac{\gamma^{-1}}{2}\|\lambda_h^{n+1} - \hat{\lambda}_h^n\|^2. \qquad (54)
\end{aligned}
$$

Then add the equations (53) and (54), multiply by $2\Delta t$ and sum over time steps to obtain

$$
\begin{aligned}
&\|e^M\|^2 + \|\epsilon^M\|^2 + \frac{(\nu-\nu_m)^2}{2(\nu+\nu_m)}\Delta t\Big(\|\nabla e^M\|^2 + \|\nabla \epsilon^M\|^2\Big) \\
&+ \frac{\nu\nu_m}{\nu+\nu_m}\Delta t\sum_{n=0}^{M-1}\left(\|\nabla e^{n+1}\|^2 + \|\nabla\epsilon^{n+1}\|^2\right) + \Delta t\sum_{n=0}^{M-1}\gamma\left(\|\nabla\cdot e_R^{n+1}\|^2 + \|\nabla\cdot\epsilon_R^{n+1}\|^2\right) \\
\leq &\Delta t\sum_{n=0}^{M-1}\frac{CC_*^2(\nu+\nu_m)}{\nu\nu_m}\left(\|e^n\|^2 + \|\epsilon^n\|^2\right) \\
&+ \Delta t\sum_{n=0}^{M-1}\gamma^{-1}\left(\|q_h^{n+1} - \hat{q}_h^n\|^2 + \|\lambda_h^{n+1} - \hat{\lambda}_h^n\|^2\right).
\end{aligned}
$$

and apply discrete Gronwall Lemma to get

$$
LHS \leq \gamma^{-1} exp\left(CC_*^2\frac{(\nu+\nu_m)}{\nu\nu_m}\right)\left(\Delta t\sum_{n=0}^{M-1}(\|q_h^{n+1} - \hat{q}_h^n\|^2 + \|\lambda_h^{n+1} - \hat{\lambda}_h^n\|^2)\right). \qquad (55)
$$

Using Lemma 4.2 with (55) yields the following desired bound:

$$
\begin{aligned}
&\Delta t\sum_{n=0}^{M-1}(\|\nabla e_R^{n+1}\|^2 + \|\nabla\epsilon_R^{n+1}\|^2) \\
&\leq C_R^2\left(\Delta t\sum_{n=0}^{M-1}\left(\|\nabla\cdot e_R^{n+1}\|^2 + \|\nabla\cdot\epsilon_R^{n+1}\|^2\right)\right) \\
&\leq \gamma^{-2}C_R^2 exp\left(CC_*^2\frac{(\nu+\nu_m)}{\nu\nu_m}\right)\left(\Delta t\sum_{n=0}^{M-1}(\|q_h^{n+1} - \hat{q}_h^n\|^2 + \|\lambda_h^{n+1} - \hat{\lambda}_h^n\|^2)\right). \qquad (56)
\end{aligned}
$$

Step 2: *Estimates of* $e_0^{n+1}, \epsilon_0^{n+1}$ *:*
To find a bound on $\left(\Delta t \sum_{n=0}^{M-1} \left(\|\nabla e_0^{n+1}\|^2 + \|\nabla \epsilon_0^{n+1}\|^2\right)\right)$, take $\chi_h = e_0^{n+1}$ in (49) and $l_h = \epsilon_0^{n+1}$ in (50) to get

$$\begin{aligned}\frac{1}{\Delta t}(e^{n+1} - e^n, e_0^{n+1}) + \frac{\nu+\nu_m}{2}\|\nabla e_0^{n+1}\|^2 = -\frac{\nu-\nu_m}{2}(\nabla \epsilon_0^n, \nabla e_0^{n+1}) \\ + (\tilde{B}_0(t^{n+1})\cdot\nabla e_R^{n+1}, e_0^{n+1}) - b^*(\epsilon^n, v_h^{n+1}, e_0^{n+1}) - b^*(\hat{w}_h^n, e_R^{n+1}, e_0^{n+1}),\end{aligned} \tag{57}$$

and

$$\begin{aligned}\frac{1}{\Delta t}(\epsilon^{n+1} - \epsilon^n, \epsilon_0^{n+1}) + \frac{\nu+\nu_m}{2}\|\nabla \epsilon_0^{n+1}\|^2 = -\frac{\nu-\nu_m}{2}(\nabla e_0^n, \nabla \epsilon_0^{n+1}) \\ + (\tilde{B}_0(t^{n+1})\cdot\nabla \epsilon_R^{n+1}, \epsilon_0^{n+1}) - b^*(e^n, w_h^{n+1}, \epsilon_0^{n+1}) - b^*(\hat{v}_h^n, \epsilon_R^{n+1}, \epsilon_0^{n+1}).\end{aligned} \tag{58}$$

Applying Cauchy-Schwarz and Hölder's inequalities with (13) on the right hand side terms of (57) and (58) yields

$$\begin{aligned}&\frac{1}{\Delta t}(e^{n+1} - e^n, e_0^{n+1}) + \frac{\nu+\nu_m}{2}\|\nabla e_0^{n+1}\|^2 \\ \le& \frac{|\nu-\nu_m|}{2}\|\nabla \epsilon_0^n\|\|\nabla e_0^{n+1}\| + C\|\tilde{B}_0(t^{n+1})\|_\infty \|\nabla e_R^{n+1}\|\|e_0^{n+1}\| \\ &+ C\left(\|\epsilon^n\|\|\nabla v_h^{n+1}\|_{L^3}\|\nabla e_0^{n+1}\| + \|\epsilon^n\|\|v_h^{n+1}\|_\infty\|\nabla e_0^{n+1}\|\right) \\ &+ C\|\nabla \hat{w}_h^n\|\|\nabla e_R^{n+1}\|\|\nabla e_0^{n+1}\|\end{aligned} \tag{59}$$

and

$$\begin{aligned}&\frac{1}{\Delta t}(\epsilon^{n+1} - \epsilon^n, \epsilon_0^{n+1}) + \frac{\nu+\nu_m}{2}\|\nabla \epsilon_0^{n+1}\|^2 \\ \le& \frac{|\nu-\nu_m|}{2}\|\nabla e_0^n\|\|\nabla \epsilon_0^{n+1}\| + C\|\tilde{B}_0(t^{n+1})\|_\infty \|\nabla \epsilon_R^{n+1}\|\|\epsilon_0^{n+1}\| \\ &+ C\left(\|e^n\|\|\nabla w_h^{n+1}\|_{L^3}\|\nabla \epsilon_0^{n+1}\| + \|e^n\|\|w_h^{n+1}\|_\infty\|\nabla \epsilon_0^{n+1}\|\right) \\ &+ C\|\nabla \hat{v}_h^n\|\|\nabla \epsilon_R^{n+1}\|\|\nabla \epsilon_0^{n+1}\|.\end{aligned} \tag{60}$$

First use Poincare's inequality with the Assumption 4.1 on the second and third right hand side terms of (59) and (60), respectively. Next, apply Young's inequality with appropriate ϵ to produce:

$$\begin{aligned}&\frac{1}{\Delta t}(e^{n+1} - e^n, e_0^{n+1}) + \frac{\nu+\nu_m}{2}\|\nabla e_0^{n+1}\|^2 \\ \le& \frac{(\nu-\nu_m)^2}{4(\nu+\nu_m)}\|\nabla \epsilon_0^n\|^2 + \frac{\nu+\nu_m}{4}\|\nabla e_0^{n+1}\|^2 + \frac{\nu\nu_m}{2(\nu+\nu_m)}\|\nabla e_0^{n+1}\|^2 \\ &+ CC_*^2\frac{\nu+\nu_m}{\nu\nu_m}(\|\epsilon^n\|^2 + \|\nabla e_R^{n+1}\|^2)\end{aligned} \tag{61}$$

and

$$\begin{aligned}
&\frac{1}{\Delta t}(\epsilon^{n+1}-\epsilon^n,\epsilon_0^{n+1})+\frac{\nu+\nu_m}{2}\|\nabla\epsilon_0^{n+1}\|^2\\
&\le\frac{(\nu-\nu_m)^2}{4(\nu+\nu_m)}\|\nabla e_0^n\|^2+\frac{\nu+\nu_m}{4}\|\nabla\epsilon_0^{n+1}\|^2+\frac{\nu\nu_m}{2(\nu+\nu_m)}\|\nabla\epsilon_0^{n+1}\|^2\\
&+CC_*^2\frac{\nu+\nu_m}{\nu\nu_m}(\|e^n\|^2+\|\nabla\epsilon_R^{n+1}\|^2). \qquad (62)
\end{aligned}$$

To evaluate the time derivative above, add and subtract the term e_R^{n+1}, and use the polarization identity. Then applying Cauchy-Schwarz, Young's and Poincare's inequalities gives us the following bound :

$$\begin{aligned}
\frac{1}{\Delta t}(e^{n+1}-e^n,e_0^{n+1})&=\frac{1}{\Delta t}(e^{n+1}-e^n,e^{n+1})-\frac{1}{\Delta t}(e^{n+1}-e^n,e_R^{n+1})\\
&\ge\frac{1}{2\Delta t}(\|e^{n+1}\|^2-\|e^n\|^2)+\frac{1}{2\Delta t}\|e^{n+1}-e^n\|^2-\frac{1}{\Delta t}(e^{n+1}-e^n,e_R^{n+1})\\
&\ge\frac{1}{2\Delta t}(\|e^{n+1}\|^2-\|e^n\|^2)-\frac{1}{2\Delta t}\|e_R^{n+1}\|^2\\
&\ge\frac{1}{2\Delta t}(\|e^{n+1}\|^2-\|e^n\|^2)-\frac{C}{2\Delta t}\|\nabla e_R^{n+1}\|^2.
\end{aligned}$$

Plugging these estimates into (61) with adding and subtracting the term $\frac{\nu\nu_m}{2(\nu+\nu_m)}\|\nabla e_0^{n+1}\|^2$ results in

$$\begin{aligned}
&\frac{1}{2\Delta t}(\|e^{n+1}\|^2-\|e^n\|^2)+\frac{(\nu-\nu_m)^2}{4(\nu+\nu_m)}\|\nabla e_0^{n+1}\|^2+\frac{\nu\nu_m}{2(\nu+\nu_m)}\|\nabla e_0^{n+1}\|^2\\
\le&\frac{(\nu-\nu_m)^2}{4(\nu+\nu_m)}\|\nabla\epsilon_0^n\|^2+CC_*^2\frac{\nu+\nu_m}{\nu\nu_m}\|\epsilon^n\|^2\\
&+C\left(C_*^2\frac{\nu+\nu_m}{\nu\nu_m}+(\Delta t)^{-1}\right)\|\nabla e_R^{n+1}\|^2. \qquad (63)
\end{aligned}$$

Using similar estimates on the right hand side terms of (62), we get

$$\begin{aligned}
&\frac{1}{2\Delta t}(\|\epsilon^{n+1}\|^2-\|\epsilon^n\|^2)+\frac{(\nu-\nu_m)^2}{4(\nu+\nu_m)}\|\nabla\epsilon_0^{n+1}\|^2+\frac{\nu\nu_m}{2(\nu+\nu_m)}\|\nabla\epsilon_0^{n+1}\|^2\\
\le&\frac{(\nu-\nu_m)^2}{4(\nu+\nu_m)}\|\nabla e_0^n\|^2+CC_*^2\frac{\nu+\nu_m}{\nu\nu_m}\|e^n\|^2\\
&+C\left(C_*^2\frac{\nu+\nu_m}{\nu\nu_m}+(\Delta t)^{-1}\right)\|\nabla\epsilon_R^{n+1}\|^2. \qquad (64)
\end{aligned}$$

Adding the equations (63) and (64), multiplying by $2\Delta t$ on both sides and summing over time steps and rearranging the terms results in

$$\begin{aligned}
&\|e^M\|^2+\|\epsilon^M\|^2+\frac{(\nu-\nu_m)^2}{2(\nu+\nu_m)}\Delta t(\|\nabla e_0^M\|^2+\|\nabla\epsilon_0^M\|^2)\\
&+\frac{\nu\nu_m}{(\nu+\nu_m)}\Delta t\sum_{n=0}^{M-1}(\|\nabla e_0^{n+1}\|^2+\|\nabla\epsilon_0^{n+1}\|^2)\le\Delta t\sum_{n=0}^{M-1}CC_*^2\frac{(\nu+\nu_m)}{\nu\nu_m}\left(\|e^n\|^2+\|\epsilon^n\|^2\right)\\
&\qquad+\Delta t\sum_{n=0}^{M-1}C\left(C_*^2\frac{(\nu+\nu_m)}{\nu\nu_m}+(\Delta t)^{-1}\right)\left(\|\nabla e_R^{n+1}\|^2+\|\nabla\epsilon_R^{n+1}\|^2\right).
\end{aligned}$$

Now drop the non-negative terms on the left hand side, apply Lemma 4.2 along with Gronwall Lemma to get

$$\begin{aligned}&\|e^M\|^2+\|\epsilon^M\|^2+\frac{\nu\nu_m}{(\nu+\nu_m)}\Delta t\sum_{n=0}^{M-1}(\|\nabla e_0^{n+1}\|^2+\|\nabla\epsilon_0^{n+1}\|^2)\\ \leq & exp\left(CC_*^2\frac{\nu+\nu_m}{\nu\nu_m}\right)CC_R^2\left(C_*^2\frac{\nu+\nu_m}{\nu\nu_m}+(\Delta t)^{-1}\right)\\ &\times\left(\Delta t\sum_{n=0}^{M-1}(\|\nabla\cdot e_R^{n+1}\|^2+\|\nabla\cdot\epsilon_R^{n+1}\|^2)\right).\end{aligned}\tag{65}$$

and then use (56) in (65), which produces

$$\begin{aligned}&\Delta t\sum_{n=0}^{M-1}\left(\|\nabla e_0^{n+1}\|^2+\|\nabla\epsilon_0^{n+1}\|^2\right)\\ &\leq\gamma^{-2}C\left(C_*^2\frac{\nu+\nu_m}{\nu\nu_m}+(\Delta t)^{-1}\right)\left(\Delta t\sum_{n=0}^{M-1}(\|q_h^{n+1}-\hat{q}_h^n\|^2+\|\lambda_h^{n+1}-\hat{\lambda}_h^n\|^2)\right)\end{aligned}\tag{66}$$

Finally, applying the triangle inequality to $(\|\nabla(v_h^{n+1}-\hat{v}_h^{n+1})\|+\|\nabla(w_h^{n+1}-\hat{w}_h^{n+1})\|)$ with

$$(a+b)^2\leq 2(a^2+b^2),\quad\forall a,b\geq 0$$

and combining the results (56) and (66) finishes the proof. □

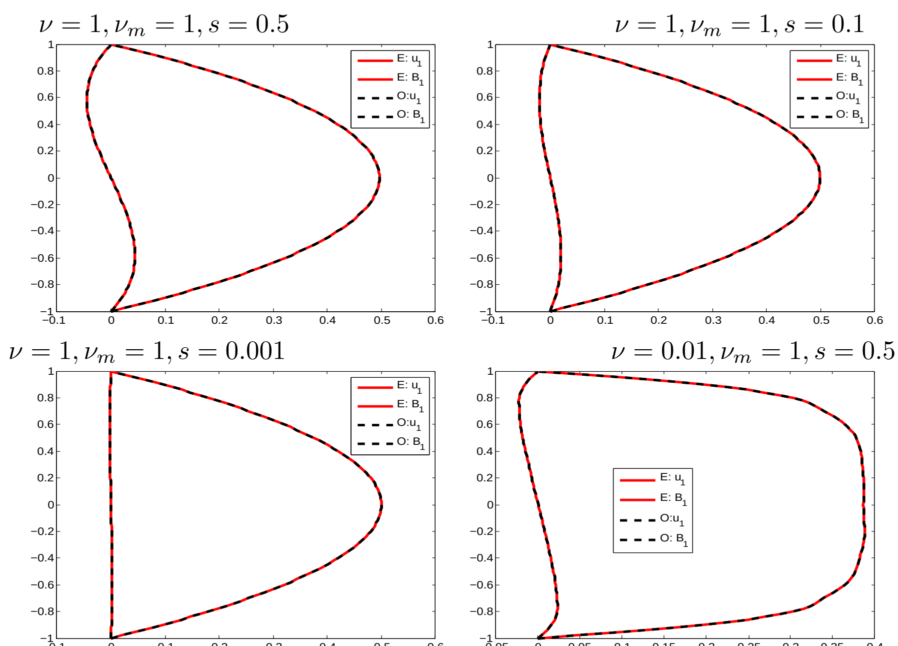

FIGURE 1. Steady state velocity and magnetic field profiles from Elsässer (E) and primitive (O) variable schemes, for various ν and s.

5. Numerical experiments

In this section, we describe the numerical experiments used to test the proposed scheme and theory above. We first verify predicted convergence rates as h and Δt goes to 0 for an analytical test problem, and then test the convergence of the penalty-projection method to the coupled scheme as $\gamma \to \infty$. We then compare computed solutions from the proposed scheme to those of a typical simulation using primitive variables for a channel flow problem. Finally, we test the proposed scheme on a test problem of channel flow over step. For all of our simulations, we choose (P_2, P_1^{disc}) Scott-Vogelius elements, which are known to be stable on barycenter refined regular triangular meshes [2]. These elements remove the effect of the (often large in MHD) pressure discretization error on the velocity/magnetic field errors.

Table 1. This table gives errors and convergence rates for analytical test problem with very small end time and varying meshwidths.

h	$dim(X_h)$	$\|v - v_h\|_{2,1}$	Rate	$\|w - w_h\|_{2,1}$	Rate
1/4	324	1.0769e-4		2.0638e-4	
1/8	1156	2.7072e-5	1.9921	5.1557e-5	2.0011
1/16	4356	6.7771e-6	1.9980	1.2887e-5	2.0003
1/32	16900	1.6949e-6	1.9995	3.2216e-6	2.0001
1/64	66564	4.2380e-7	1.9997	8.0541e-7	2.0000

5.1. Numerical experiment 1: Convergence as $h, \Delta t \to 0$.

We now test the predicted convergence rates of our analysis, for the mesh width h and timestep Δt tending to 0. We picked the analytical solution

$$v = \begin{pmatrix} \cos y + (1+e^t)\sin y \\ \sin x + (1+e^t)\cos x \end{pmatrix},\; w = \begin{pmatrix} \cos y - (1+e^t)\sin y \\ \sin x - (1+e^t)\cos x) \end{pmatrix},\; p = -\lambda = \sin(x+y),$$

domain $\Omega = (0,1)^2$, $\nu = \nu_m = 1$, and compute f_1 and f_2 from this. We then computed with Algorithm 3.1, and compared our computed solution with this known analytical solution. Recall our analysis predicts that

$$\|v - v_h\|_{2,1} + \|w - w_h\|_{2,1} \le C(\Delta t + h^2)$$

for this element choice, with $\|\phi\|_{2,1} := \|\phi\|_{L^2(0,T;H^1(\Omega)^d)}$.

To test the spatial convergence rate, we select a small end time $T = 0.001$, timestep $\Delta t = T/8$, and compute on successively refined meshes. Errors and rates are shown in table 1, and we observe second order spatial convergence, which is in agreement with our analysis. To test the temporal convergence rate, we use a mesh width of $h = 1/64$, end time $T = 1$, and compute with varying timestep sizes. Errors and rates are shown in Table 2, and the expected first order temporal convergence is observed.

5.2. Numerical experiment 2: Convergence of penalty-projection scheme to coupled scheme as $\gamma \to \infty$.

In Section 4, we proposed a variation on Algorithm 3.1 that uses a penalty-projection method for each decoupled problem. This is typically more efficient, as the linear systems that arise are much easier to solve. However, accuracy in projection type methods is often an issue, but we prove in Section 4 that with large enough penalty parameter, the penalty-projection scheme

TABLE 2. This table gives errors and convergence rates for analytical test problem with a fine mesh, large end time and varying timestep size.

Δt	$\|v - v_h\|_{2,1}$	Rate	$\|w - w_h\|_{2,1}$	Rate
$T/1$	4.1088e-2		4.0721e-2	
$T/2$	2.0206e-2	1.0239	1.9987e-2	1.0267
$T/4$	9.9334e-3	1.0244	9.8156e-3	1.0259
$T/8$	4.9141e-3	1.0154	4.8534e-3	1.0161
$T/16$	2.4430e-3	1.0083	2.4123e-3	1.0086
$T/32$	1.2181e-3	1.0040	1.2029e-3	1.0040

TABLE 3. Shown above are the differences between the penalty-projection and coupled schemes, for varying γ.

γ	$\|v - \hat{v}\|_{\infty,1}$	rate	$\|\nabla \cdot v\|_{\infty,0}$	$\|w - \hat{w}\|_{\infty,1}$	rate	$\|\nabla \cdot w\|_{\infty,0}$
0	4.00e-1	–	2.807e-1	3.663e-1	–	2.676e-1
1	3.041e-1	0.1196	1.996e-1	2.727e-1	0.1280	1.874e-1
10	1.083e-1	0.4481	6.451e-2	9.352e-2	0.4649	5.854e-2
10^2	1.507e-2	0.8567	8.653e-3	1.277e-2	0.8645	7.744e-3
10^3	1.571e-3	0.9819	2.676e-4	1.327e-3	0.9833	8.015e-4
10^4	1.578e-4	0.9982	9.007e-5	1.578e-4	0.9983	8.043e-5

gives the same solution as Algorithm 3.1, since Theorem 4.1 proves it converges to this method as $\gamma \to \infty$.

To test this convergence, we pick right hand sides f_1 and f_2 and initial conditions corresponding to chosen solution

$$v = \begin{pmatrix} \sin(2\pi y) \\ \cos(2\pi x) \end{pmatrix} \exp(t),\ w = \begin{pmatrix} \cos(\pi y) \\ \sin(\pi x) \end{pmatrix} \exp(t),\ q = r = \sin(\pi(x+y))(1+t),$$

with $\nu = 1, \nu_m = 1$. On a h=1/16 barycenter refined triangulation of a domain $\Omega = (0,1) \times (0,1)$, with $T = 1$, and $\Delta t = 0.1$. We then compute with both the coupled scheme formulation of Algorithm 3.1 and with the penalty-projection scheme formulation of Algorithm 4.1, with varying γ. We then calculated the differences in solutions, and associated rates. These are shown in Table 3, and show the predicted first order convergence. Note that since the timestep size is fixed, we used the more convenient L^∞ norm in time (i.e. we needed only to compare the solutions at the last timestep).

5.3. Numerical experiment 3: Comparison of proposed Elsässer variable scheme to primitive variable scheme. Next, we compare the proposed scheme against a typical scheme for primitive variable MHD, which is given in the case of homogeneous Dirichlet boundary conditions by: Find $(u_h^n, p_h^n, B_h^n, \lambda_h^n) \in X_h \times Q_h \times$

$X_h \times Q_h$ such that

$$\frac{1}{\Delta t}(u_h^{n+1} - u_h^n, v_h) + b^*(u_h^n, u_h^{n+1}, v_h) - (p_h^{n+1}, \nabla \cdot v_h)$$
$$+\nu(\nabla u_h^{n+1}, \nabla v_h) - sb^*(B_h^n, B_h^{n+1}, v_h) = (f, v_h), \tag{67}$$
$$(\nabla \cdot u_h^{n+1}, r_h) = 0, \tag{68}$$
$$\frac{1}{\Delta t}(B_h^{n+1} - B_h^n, \chi_h) + b^*(u_h^n, B_h^{n+1}, \chi_h) - b^*(B_h^n, u_h^{n+1}, \chi_h)$$
$$-(\lambda_h^{n+1}, \nabla \cdot \chi_h) + \nu_m(\nabla B_h^{n+1}, \nabla \chi_h) = (\nabla \times g(t^{n+1}), \chi_h), \tag{69}$$
$$(\nabla \cdot B_h^{n+1}, \rho_h) = 0, \tag{70}$$

for every $(v_h, r_h, \chi_h, \rho_h) \in X_h \times Q_h \times X_h \times Q_h$. In the case of non homogeneous Dirichlet boundary conditions, the usual change to the solution spaces is made. We believe this is a fair comparison to make, since this scheme is an unconditionally stable linearized backward Euler scheme, just as the proposed Elsässer variable scheme in Algorithm 3.1 is. Of course, the proposed Elsässer variable is much more efficient, since it decouples the problem. It is an open problem how to decouple a primitive variable MHD system in an unconditionally stable way.

For this comparison of schemes, we consider channel flow on a 10×40 rectangle, with initial condition $B = 0$ and $u =< (1-y^2)/2, 0 >$. These initial conditions also define the inflow/outflow conditions for all $t > 0$. On the upper and lower walls, no slip conditions are enforced for velocity, and a magnetic field $B =< 0, 1 >$ is enforced. The magnetic diffusivity constant is selected as $\nu_m = 1$. The coupling number s and the kinematic viscosity ν are varied in the tests. For all tests, a steady state was reached by $T = 40$ (using timesteps of $\Delta t = 0.05$, and shown in Figure 1 are velocity and magnetic field steady state profiles at $x = 20$ for both schemes. A barycenter refined mesh that provided a total of 24,756 degrees of freedom was used.

From the plots, we observe excellent agreement in the solutions of the primitive and Elsässer variable schemes for each choice of s and ν, as the plots of the profiles lie on top of each other. We note that several other variations of $\nu,\ \nu_m,\ s$ were made, and in all cases the profile plots of solutions of primitive and Elsässer variable schemes had excellent agreement.

5.4. Numerical experiment 4: MHD Channel Flow over a step. For our final numerical experiment, we test Algorithm 3.1 on two dimensional channel flow over a forward and backward facing step in the presence of a magnetic field, with $\nu = 0.001$ and $\nu_m = 1$. It is expected that as the strength of the magnetic field grows, transient behavior will be damped, and the velocity flow profile will change from parabolic to nearly plug-like (away from the step), similar to the previous example.

We choose a domain that is a 30×10 rectangle with a 1×1 step five units into the channel at the bottom. We enforce boundary conditions for v and w that correspond to no slip velocity and $B = \langle 0, 1\rangle^T$ on the walls and step, and $u = \langle y(10-y)/25, 0\rangle^T$ at the inflow, $B = 0$ at the inflow and outflow, and with outflow conditions for u. The initial conditions are $\tilde{B}_0 = 0$ and $u_0 = \langle y(10-y)/25, 0\rangle^T$. Computations are run to $T = 40$, using a timestep of $\Delta t = 0.025$ and a mesh that provided $568,535$ total degrees of freedom. Plots for the solutions with $s = 0,\ 0.01$ and $s = 0.05$ are shown at T=40 in Figure 2. We observe as s increases, the shedding of eddies behind the step is inhibited, and the change in velocity profile is clearly altered

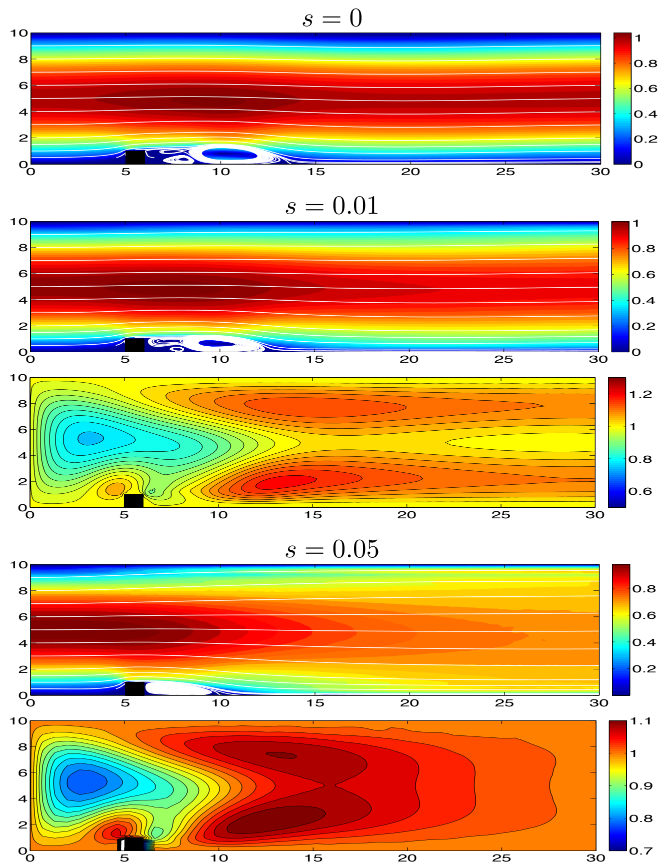

FIGURE 2. Shown above are T=40 velocity solutions (shown as streamlines over speed contours) for MHD Channel flow over a step with varying s, and associated magnetic field magnitudes.

away from a parabolic shape. The magnetic field plots show a clear interaction between the flow and induced magnetic field which changes the magnetic field.

6. Conclusions and future directions

We have proposed, analyzed and tested an efficient, fully discrete numerical scheme for MHD. By formulating with Elsässer variables, unconditionally stability is proven in a decoupled algorithm (decoupling of the 4-equation, 4-unknown system into 2-equation, 2-unknown systems). Unconditional stability with respect to meshwidth and timestep size are also proven. Moreover, a more efficient penalty-projection method for each 2-equation system, and this method is proven to be equivalent to the 2-equation, 2-unknown scheme for large penalty parameters.

Results of several successful numerical experiments were presented. Convergence rates to a chosen analytical solution were found to be optimal, which is in agreement with our analysis. Convergence of the penalty-projection scheme to the 2-equation, 2-unknown scheme was found to be first order as $\gamma \to \infty$, which agrees with our theory. Two channel flow problems were also studied. The first was a comparison of the Elsässer scheme solution to that of primitive variable MHD, for a variety of viscosities and coupling numbers, and in each case excellent agreement between the solutions was found. Finally, we testing MHD channel flow over a step, and observed the changing of physical behavior as the coupling number increased.

For future work, we believe that more testing of the scheme needs performed. If it can be established that this scheme gives solutions very similar to primitive variable schemes with the same mesh and timestep on a wide variety of problems, then the proposed schemes (or perhaps variants of them) could be an enabling tool to simulate larger scale 3D problems than is currently possible. Also, for MHD problems with higher Reynolds number, reduced order modeling with large eddy simulation, in the context of the scheme proposed herein, should be explored.

Acknowledgements

This research was supported by National Science Foundation grant DMS1112593 (MM and LR) and TUBITAK (MB and SK)

References

[1] Ph. Angot, M. Jobelin, and J. Latche. Error analysis of the penalty-projection method for the time dependent Stokes equations. Int. J. Finite Vol., 6:1–26, 2009.
[2] D. Arnold and J. Qin. Quadratic velocity/linear pressure Stokes elements. In R. Vichnevetsky, D. Knight, and G. Richter, editors, Advances in Computer Methods for Partial Differential Equations VII, pages 28–34. IMACS, 1992.
[3] L. Barleon, V. Casal, and L. Lenhart. MHD flow in liquid-metal-cooled blankets. Fusion Engineering and Design, 14:401–412, 1991.
[4] J.D. Barrow, R. Maartens, and C.G. Tsagas. Cosmology with inhomogeneous magnetic fields. Phys. Rep., 449:131–171, 2007.
[5] D. Biskamp. Magnetohydrodynamic Turbulence. Cambridge University Press, Cambridge, 2003.
[6] P. Bodenheimer, G.P. Laughlin, M. Rozyczka, and H.W. Yorke. Numerical methods in astrophysics. Series in Astronomy and Astrophysics, Taylor & Francis, New York, 2007.
[7] S.C. Brenner and L.R. Scott. The Mathematical Theory of Finite Element Methods, volume 15 of Texts in Applied Mathematics. Springer-Verlag, New York, 1994.
[8] P. A. Davidson. An introduction to magnetohydrodynamics. Cambridge Texts in Applied Mathematics, Cambridge University Press, Cambridge, 2001.
[9] M. Dobrowolny, A. Mangeney, and P. Veltri. Properties of magnetohydrodynamic turbulence in the solar wind. Astron. Astrophys., 83:26–32, 1980.
[10] E. Dormy and A.M. Soward. Mathematical aspects of natural dynamos. Fluid Mechanics of Astrophysics and Geophysics, Grenoble Sciences. Universite Joseph Fourier, Grenoble, VI, 2007.
[11] W. M. Elsässer. The hydromagnetic equations. Phys. Rev., 79:183, 1950.
[12] J. A. Font. Gerneral relativistic hydrodynamics and magnetohydrodynamics: hyperbolic system in relativistic astrophysics, in hyperbolic problems: theory, numerics, applications. Springer, Berlin, pages 3–17, 2008.
[13] V. Girault and P.-A.Raviart. Finite element methods for Navier-Stokes equations: Theory and Algorithms. Springer-Verlag, 1986.
[14] V. Girault and P.-A. Raviart. Finite element approximation of the Navier-Stokes equations, volume 749 of Lecture Notes in Mathematics. Springer-Verlag, Berlin, 1979.
[15] H. Hashizume. Numerical and experimental research to solve MHD problem in liquid blanket system. Fusion Engineering and Design, 81:1431–1438, 2006.
[16] J.G. Heywood and R. Rannacher. Finite-element approximation of the nonstationary navier-stokes problem part iv: error analysis for second-order time discretization. SIAM J.Numer. Anal., 27:353–384, 1990.
[17] W. Hillebrandt and F. Kupka. Interdisciplinary aspects of turbulence. Lecture Notes in Physics, Springer-Verlag, Berlin, 756, 2009.
[18] M. Jobelin, C. Lapuerta, J.-C. Latche, Ph. Angot, and B. Piar. A finite element penalty-projection method for incompressible flows. Journal of Computational Physics, 217:502–518, 2006.
[19] L.D. Landau and E.M. Lifshitz. Electrodynamics of Continuous Media. Pergamon Press, Oxford, 1960.

[20] W. Layton. Introduction to the Numerical Analysis of Incompressible Viscous Flows. SIAM, 2008.

[21] A. Linke, M. Neilan, L. Rebholz, and N. Wilson. A connection between coupled and penalty projection timestepping schemes with FE spacial discretization for the Navier-Stokes equations. submitted, 2014.

[22] E. Marsch and C.-Y. Tu. Dynamics of correlation functions with Elsässer variables for inhomogeneous MHD turbulence. J. Plasma Phys., 41:479–491, 1989.

[23] B. Punsly. Black hole gravitohydrodynamics. Astrophysics and Space Science Library, Springer-Verlag, Berlin, Second Edition, 355, 2008.

[24] J. Qin and S. Zhang. Stability and approximability of the P1-P0 element for Stokes equation. International Journal for Numerical Methods in Fluids, 54:497–515, 2007.

[25] P. Schmidt. On a magnetohydrodynamic problem of Euler type. Journal of Differential Equations, 74:318, 1988.

[26] S.Smolentsev, R.Moreau, L.Buhler, and C.Mistrangelo. MHD thermofluid issues of liquid-metal blankets: Phenomena and advances. Fusion Engineering and Design, 85:1196–1205, 2010.

[27] C. Trenchea. Unconditional stability of a partitioned IMEX method for magnetohydrodynamic flows. Applied Mathematics Letters, 27:97–100, 2014.

[28] N. Wilson, A. Labovsky, and C. Trenchea. High accuracy method for magnetohydrodynamics system in Elsässer variables. Computational Methods in Applied Mathematics, to appear, 2014.

[29] S. Zhang. A new family of stable mixed finite elements for the 3d Stokes equations. Mathematics of Computation, 74:543–554, 2005.

[30] S. Zhang. Quadratic divergence-free finite elements on Powell-Sabin tetrahedral grids. Calcolo, 48(3)211–244, 2011.

Department of Mathematics, Middle East Technical University, Ankara, Turkey, 06531
E-mail: miakbasb@metu.edu.tr

Department of Mathematics, Middle East Technical University, Ankara, Turkey, 06531
E-mail: smerdan@metu.edu.tr

Department of Mathematical Sciences, Clemson University, Clemson, SC, 29634
E-mail: mmohebu@clemson.edu

Department of Mathematical Sciences, Clemson University, Clemson, SC, 29634
E-mail: rebholz@clemson.edu